ITERATIVE INVERSION FOR TOPOLOGY MAPPING OF BRANCHED NETWORKS USING TIME DOMAIN REFLECTOMETRY

by

Steven Michael Smith

A thesis submitted to the faculty of
The University of Utah
in partial fulfillment of the requirements for the degree of

Master of Science

in

Electrical Engineering

Department of Electrical and Computer Engineering

The University of Utah

December 2007

Copyright © Steven Michael Smith 2007

All Rights Reserved

THE UNIVERSITY OF UTAH GRADUATE SCHOOL

SUPERVISORY COMMITTEE APPROVAL

of a thesis submitted by

STEVEN MICHAEL SMITH

This thesis has been read by each member of the following supervisory committee and by majority vote has been found to be satisfactory.

Chair: Furse

M. S. Zhdanov

THE UNIVERSITY OF UTAH GRADUATE SCHOOL

FINAL READING APPROVAL

To the Graduate Council of the University of Utah:

I have read the thesis of STEVEN MICHAEL SMITH in its final form and have found that (1) its format, citations, and bibliographic style are consistent and acceptable; (2) its illustrative materials including figures, tables, and charts are in place; and (3) the final manuscript is satisfactory to the supervisory committee and is ready for submission to The Graduate School.

Date

Cynthia Furse
Chair: Supervisory Committee

Approved for the Major Department

Marc Bodson
Chair/Dean

Approved for the Graduate Council

David S.
Dean of The Graduate School

ABSTRACT

Branched wiring networks are interconnections of wires that provide for the connection of dc and RF (Radio Frequency) components in an aircraft or other type of apparatus or structure. If by age or by mechanical means the wiring network develops a wiring fault such as bare wire, it can cause fire or other types of emergencies which may cause the loss of life and or property.

A Steepest Descent Method is applied to the determination of the topology of a network of branched wires from the Time Domain Reflectometry (TDR) response of the network. Inversion theory is used to derive the equations necessary for the Steepest Descent Method. Functional Spaces are explained, and the properties of the Hilbert Space are used in the minimization of the Misfit Functional. A computer algorithm is written taking into account all a priori information so as to speed the process of finding the wire topology map.

The method works reasonably well if the data are perfect (no noise). With the addition of noise the algorithm needs to be modified. Noise causes the impedance values to spread, making the determination of characteristic impedance more problematic.

To my wife Lethia for all her support, patience and love

and to our children Gregory and Veronica

CONTENTS

LIST OF FIGURES

CHAPTER 1

INTRODUCTION

Much research has been done to determine viable reflectometry methods for the location of wiring faults. This effort has been spurred on by catastrophic accidents in the commercial aviation industry, fires in public buildings, and other problems caused by wiring failures. As aircraft age, the risk they pose to those flying and to those present at ground zero make their upkeep and maintenance a public concern. In addition the building industry has had a number of electrical fires that have caused the deaths of many.

A reliable method for locating wiring problems is needed for the safety of the general public. With life and limb at stake, the expense of maintaining faulty wiring is a driving force in funding the development of better fault location methods. Currently, several methods are available to determine wire fault locations. These methods all have their own limitations. Some use high voltages and therefore are unsuitable for use on fueled aircraft.[1] Others require a great deal of equipment and expensive to implement.[1] Some methods require technical expertise to understand and analyze the data.

Among these methods are Time Domain Reflectometry (TDR), Frequency Domain Reflectometry (FDR), Mixed Signal Reflectometry (MSR), Sequence Time Domain Reflectometry (STDR), Spread Spectrum Time Domain Reflectometry (SSTDR), and Capacitance and Inductance Sensors. All of these methods (except capacitance and inductance sensing) send a high frequency signal down the line, and evaluate the reflected signal to locate a fault in the wiring. The signals and the process of analysis differ between each method, but the results are similar. A reflection is observed at every impedance discontinuity. The magnitude of the reflection is related to the impedance change by:

$$|\Gamma| = \left| \frac{V_{\text{Ref}}}{V_{\text{Inc}}} \right| = \left| \frac{Z - Z_o}{Z + Z_o} \right| \tag{1.1}$$

The signal transmitted through the discontinuity has a magnitude of

$$|T| = \left| \frac{V_{\text{Trans}}}{V_{\text{Inc}}} \right| = \left| \frac{2Z}{Z + Z_o} \right| \tag{1.2}$$

T = Transmission Coefficient

The time delay between the incident signal and the reflection is proportional to the distance to the impedance discontinuity:

$$t_{delay} = \frac{2d\sqrt{\varepsilon_r}}{c} \quad \text{(seconds)} \tag{1.3}$$

d = Distance to the Discontinuity (meters)
ε_r = Relative Dielectric Constant of the Propagation Medium
c = Speed of Light in Free Space (meters/second)

The equation may be easier to understand in a slightly modified form

$$t_{delay} = \frac{2d}{\left(\frac{c}{\sqrt{\varepsilon_r}}\right)} \tag{1.4}$$

which shows that the delay is the distance to the discontinuity and back (hence the factor of 2) divided by the speed at which the wave travels in the medium.

Reflections are bilinearly related to the impedance discontinuity and are largest when the discontinuities are largest. Open and short circuits provide a total reflection (in phase and out of phase, respectively) of the impinging wave on the termination (open/short). When the impedance discontinuity is small, so is the reflection from the discontinuity. This can be so small that the reflection falls below the noise level of the measuring equipment, rendering the discontinuity invisible.[2]

1.1 Time Domain Reflectometry (TDR)

A Time Domain Reflectometer (TDR) is a device that measures the reflection of a

voltage wave from a voltage step function incident on a network. The key to understanding the TDR measurement is that it only measures the reflected voltage at the probe location. Many sources of reflection exist even in a very simple wiring system, as shown in Figure 1-1. Assuming that all impedances are different ($Z_G \neq Z_o \neq Z_L$), there is an impedance discontinuity at each interface in the test setup and within the wiring network. In Figure 1-1 there are two impedance discontinuities where there is an impedance change. The first discontinuity is where Z_G meets Z_o, and the other is where Z_o meets Z_L (both designated as doted lines in Figure 1-1). At each discontinuity there will be a reflection, the magnitude and phase of which will depend on the direction from which the

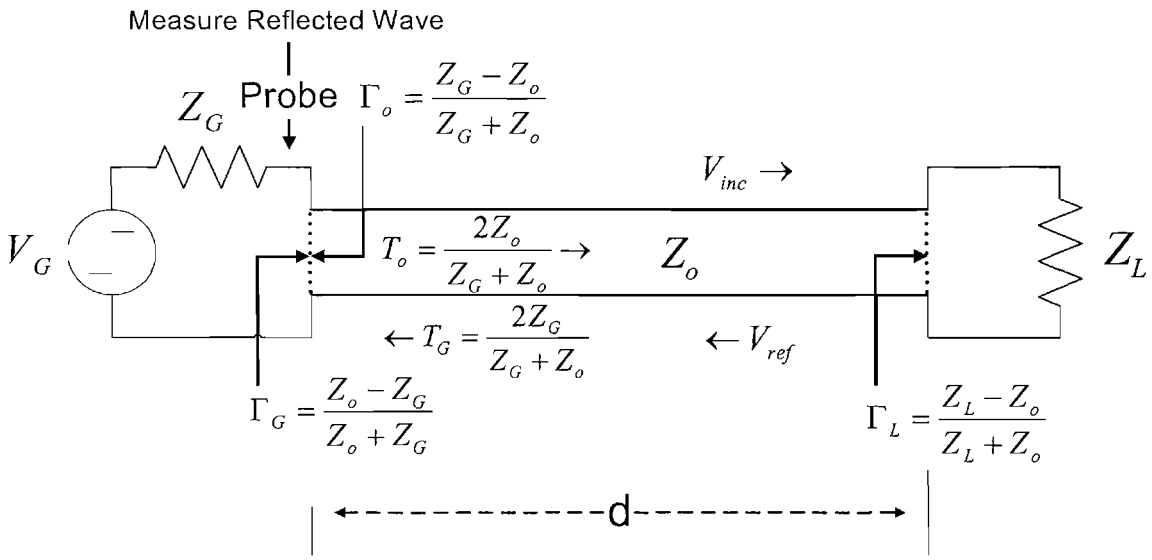

Figure 1-1 Basic TDR Measurement Setup

voltage wave is coming and the relative impedances. So as not to make the diagram too busy, Figure 1-1 only shows the initial reflections and transmission coefficients. Multiple reflections do occur as the waves reverberate within the system.

The signal is transmitted to the transmission line through Z_G. When the signal hits the transmission line, a reflection occurs, reflecting a voltage back towards the generator with a magnitude of $V_G\Gamma_G$. This voltage is picked up by the TDR probe shown in the figure. The rest of the voltage wave ($V_G T_o = V_{inc}$) is transmitted through the interface to the transmission line. V_{inc} continues to travel along the transmission line towards the load at a velocity of $\frac{c}{\sqrt{\varepsilon_r}}$ (meters per second). When V_{inc} reaches the load, another reflection occurs. A portion of V_{inc} is reflected back towards the source end of the wiring network with a value of $V_{inc}\Gamma_L$. The reflected wave continues to travel toward the source end of the wiring network and again sees the impedance discontinuity at the interface between the source and the wire. $V_{inc}\Gamma_L T_G$ is transmitted to the probe. At the probe the voltage is the sum of the initial reflection $V_G\Gamma_G$ and $V_{inc}\Gamma_L T_G$. The reflected wave at the source would now be $V_{inc}\Gamma_L\Gamma_G$ and would continue being reflected and transmitted on the transmission line until all reflections die out below the noise level of the measurement system.

1.2 Wiring Faults

Faults produce impedance discontinuities in wiring networks, and these changes are what we wish to detect with reflectometry methods. Open ($Z=\infty$) and short ($Z=0\Omega$) circuits produce large reflections ($\|\Gamma\|=1$) that can generally be located by all of today's reflectometry methods. Chafes or frays produce reflections that are generally too small to locate, because their reflections are smaller than those caused by vibration, moisture on the wire, etc.[2] There is normally a reflection at the junction between the test cable and the network being tested, which overshadows other reflections from faults very near the start of the wire. This "blind zone" is common to all reflectometry methods, although the exact length depends on the specifics of the test system. Wire junctions also produce complex reflections when additional reflections are created as the signals reverberate within the network.

Analysis of impedance changes due to branched wires has challenges beyond those of more simple faults. First, branches place two or more wires in parallel, reducing the overall impedance seen at the junction. An example of this would be two wires at a branch with characteristic impedances of 100Ω each, producing an impedance of 50Ω at the junction. Reflections that are small or nonexistent could fall below the noise level of the testing system and would therefore remain unseen. Second, branches make pinpointing the fault location difficult. The distance to the fault may be determined, but it may not be clear which branch it is on. The problem of locating faults on branched networks is what this thesis seeks to address.

Recall that the TDR measurement only measures the reflected voltage returned at the source end of a wiring network. Figure 1-2 demonstrates the traditional "bounce diagram" method of calculating TDR signatures. The wire network is represented at the top of the figure, and the left most part of the figure shows the TDR response. The right part of Figure 1-2 is the bounce diagram of the same wiring network. (The figure has been simplified to make it easier to follow.)

The diagram has been labeled in meters instead of time (using the velocity of propagation to calculate these distances) to show that the voltage wave travels through the transmission line, and then a portion of the wave is reflected back at each discontinuity of the network back towards the other end. These reflections occur at each and every discontinuity. Again, the returning voltage waves are summed as they are detected at the TDR measurement device located at the input to the wiring network.

1.3 Summary

Chapter 2 discusses the problems and limitations of TDR measurements, and the assumptions that were used in this work. Inversion theory is discussed, and the various methods of steepest descent are presented.

Chapter 3 describes in more detail the forward operator and the Frechet derivative. Analysis of the functional space is performed, and the impact of using difference equations to compute the Frechet derivative is discussed. Plots of the functional space show the geometry that is set up by the misfit functional and that this

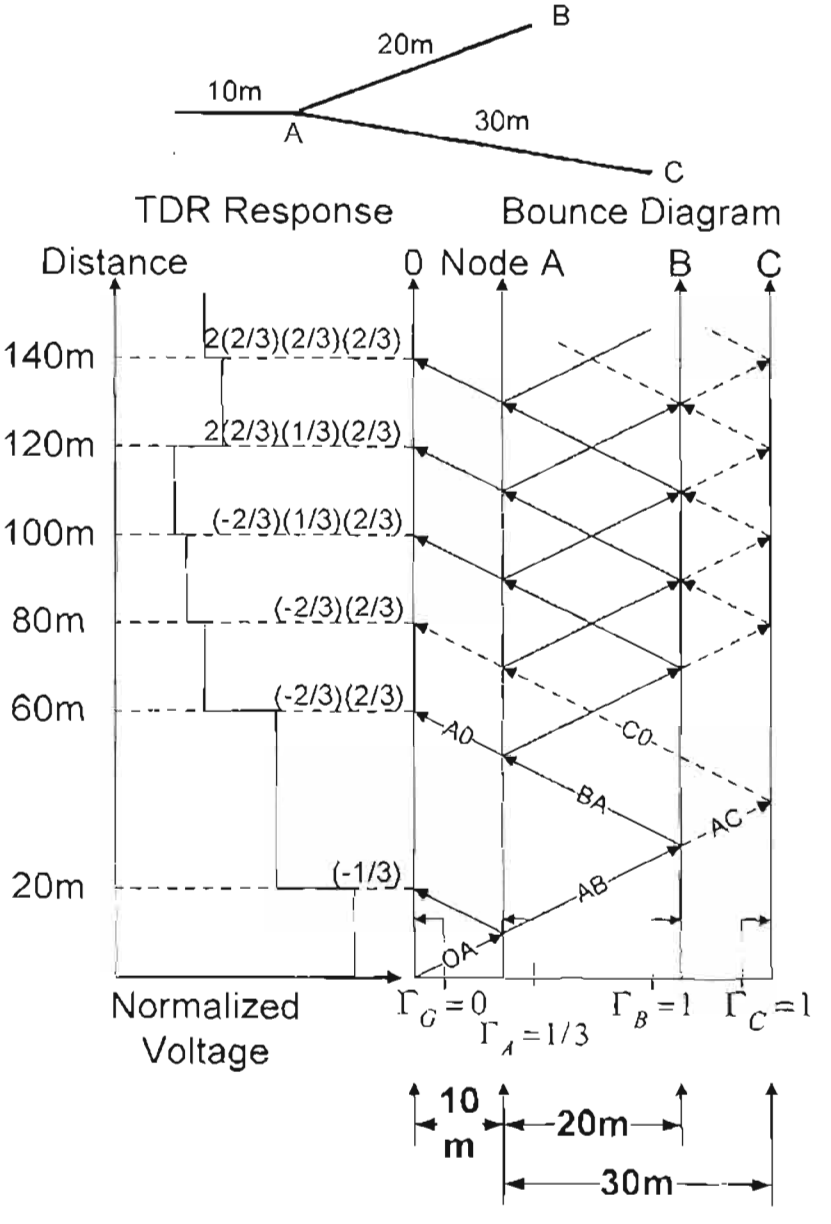

Figure 1-2 Bounce Diagram with TDR Response

geometry can be exploited in determining the wire map from the input TDR data.

Chapter 4 shows how the steepest descent method was used in finding the wiring network mapping given the input TDR data. Results are discussed and presented. The computer algorithm is illustrated by example.

The Appendix gives properties of different spaces and some mathematical background that may make it easier to follow the derivation of the various methods of minimization.

CHAPTER 2

THE PROBLEM: BRANCHED NETWORKS

The goal of this effort is to develop a method for mapping a branched wiring topology given the Time Domain Reflectometry (TDR) response. Raw TDR data can be quite complicated and very difficult to read because of the multiple reflections from a branched network. Figure 1-2 showed a ``bounce diagram`` representation of the reflections and multiple reflections on a simple ``Y`` network and the TDR response seen at the input. Even for this relatively simple network, it would be extremely difficult to read and interpret this plot to determine the ``Y`` network topology.

An automated method of analyzing the data and displaying the network topology is needed. This would allow quick discovery of the location of defects in the wiring network. The wiring could then be repaired in a timely fashion, saving lives, time, and expense.

In this research, several assumptions are made: (1) Loads will be restricted to opens and shorts. It would also be possible to do this analysis if the loads were other than open or short, as long as they were specified in advance. This is generally a good assumption for many types of faults. Wires connected to capacitive or inductive loads

cannot be analyzed. Therefore, the user may need to disconnect these types of loads before testing, leaving the ends of the wires open. The number of branches at any junction is assumed to be 3 or less. This appears to be a reasonable assumption based on the few aircraft wiring diagrams that have been obtained.

The characteristic impedance, Z_o , will be $50\Omega, 75\Omega, 125\Omega, 200\Omega - 300\Omega$ (where $Z_o/3$ will range from 48Ω to 54Ω). This is based on the types of wires typically used in aircraft.

The structure of the network is not known in advance, but the limiting structure is show in Figure 2-1. The measured TDR response is assumed to be given.

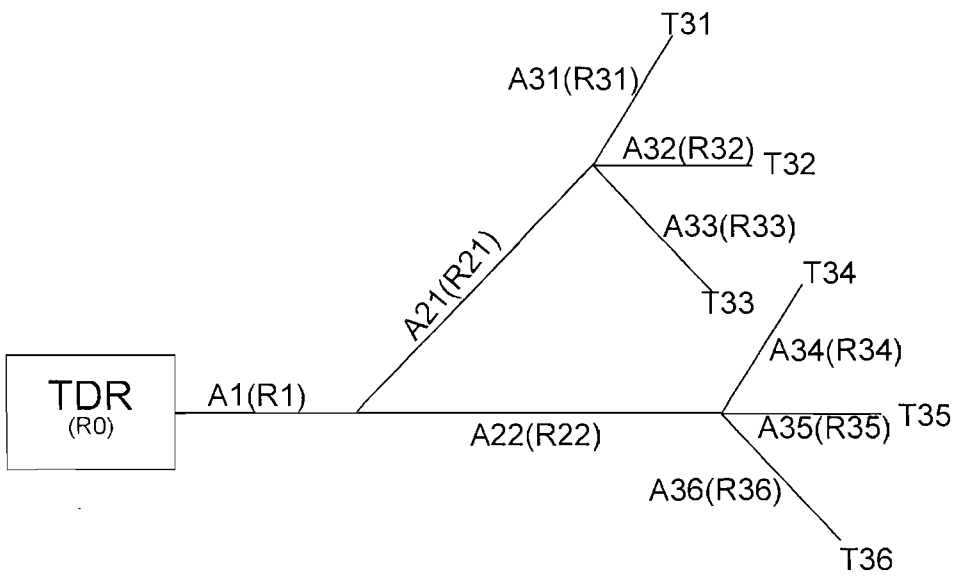

Figure 2-1 Maximum Structure Size and Topology

2.1 Other Methods

Two methods have previously been developed to define the network topology from reflectometry data.

A "brute force" method was used in [4]. In [4], every conceivable wiring configuration was simulated to find the one that best fits the data. The range of "conceivable" configurations can be limited to combinations of lengths where the impulse response of the reflectometry signal is nonzero, which makes this a feasible and a functional method. It is very cumbersome, however, and highly prone to error for measured data where the impulse response is imperfect.[3]

A genetic algorithm has also been tested to map the topology of a branched network. The genetic algorithm uses a random generation of possible network configurations, tending towards the best fit. This method could conceivably be more noise tolerant. However this has not been found to be the case, and the genetic algorithm solution does not work as well as the brute force method.[4]

2.1.1 Our Method

A method based on nonlinear optimization or inversion will be applied in this thesis to determine the network topology. A significant advantage of this method is the ability to quantify the quality of the calculated solution and area of ambiguity within the data. This will be done by defining the problem in such a way as to allow the use of a Hilbert space. Hilbert spaces have special properties that permit the determination of the distance between the measured and predicted data, as well as the slope of the misfit

functional to determine the closeness of the proposed solution to the measured data. With this information, a determination of the fastest way to find the solution to the wiring configuration can be programmed. The method is robust enough to find the network topology even in the presence of noisy data. It is also hoped that it will be able to provide a prediction of the confidence level of the solution.

Several approximations were required:

1. Ideal, numerically generated data were used to aid in the design and testing of the algorithm.
2. A priori information on the extent (maximum number of wires and branches) of the network topologies present in the model space was used to restrict the size of the correctness set.
3. Impedances of allowed discontinuities are used in determining a correctness set. This would influence how many wires would be added at a branch junction and their characteristic impedances.

2.2 Objective

The objective of this thesis is to use regularization theory and real analysis to obtain the inverse operator for the TDR response of a branched network with minimal computational time and good accuracy.

2.3 Inversion Theory

Inversion Theory has been used extensively in exploring the earth's crust and the

universe in which we live. Geophysicists have used seismic soundings, gravitational variation, electrical and electromagnetic measurements to measure what the earth is made of and where mineral and oil deposits can be found under the surface of the earth. Geophysicists collect these data and from the data extract information on the phenomena that caused the effects seen in the measured data.[5]

There is a small bit of the terminology used in inversion theory that needs to be understood to follow what will be presented next, i.e., forward operator, inversion, functional, Model space, Data space, Correctness Set, and a priori information. Inversion theory sets up the problem in a geometry that allows the minimization of a misfit functional. This geometry is found in a Hilbert Space. All of this will be explained in the following sections.

2.3.1 Hilbert Space

Hilbert spaces are complete normed linear spaces with a defined inner product. Complete means that the boundary is part of the Hilbert space and any sequence will terminate on an object that is contained within the same space. A normed space allows for a distance to be defined between objects of the space. Linear spaces allow for mathematical operations to be performed on objects within the space, and the end results will still lie within the same space. The inner product defines a direction between the objects of the space. The inner product has many of the same properties as the inner product of a 3D vector space. With the properties of distance and direction found between elements of the Hilbert space, sequences can then be found that bring parameters

of the input vector arbitrarily close to the parameters that created the measured data. This allows the space containing the model to be connected to the space containing the data through the forward operator, both of which are Hilbert spaces. These properties define a special geometry for our functional space, which can be exploited for the minimization problem.

Consider the forward operator $A(*)$. This operator is a function that takes the input parameters such as the kind of minerals and where they are located under the ground, and with these parameters generates the data that we would expect to obtain with measuring equipment. A typical forward operator would be an analytical or numerical approach to compute the electric or magnetic fields (the data) from a layered model of the earth (the model). Inversion of an operator is a method of finding the input to the operator, the model, from the measured output data. For example, given measured electric field data, the geometry of the earth (model $\mathbf{m}$) is found using the FDTD forward operator. With the Forward Operator $A(*)$ and the data $\mathbf{d}$ known, the input $\mathbf{m}$ can be found. This is called inversion. For this thesis, bold letters denote vectors.

A functional is a function that takes two vectors (or some other type of object) and integrates them with a generalized function such as the Kroneker delta function $\delta(x)$ and returns a number. For this application, the measured and computed data are compared through a functional to determine a real number that indicates the closeness of the two data points.

The model space M contains inputs to the operator $A(*)$, so the elements of M are

the $\mathbf{m}_n$ model vectors. For this thesis application, the model vectors are a representation of the wire network. Through this forward operator the M space (wire network parameters) can be mapped into the data D space (TDR response). The data space contains vectors that represent the measured reflectometry responses of wiring networks. The mapping of sequences of $\mathbf{m}_n$ into the D space produces sequences of $\mathbf{d}_n$ vectors. As the estimated model $\mathbf{m}_n$ approaches the real model $\mathbf{m}$, the misfit functional becomes smaller and smaller as $n \to \infty$ for any $\varepsilon > 0$. The closeness of the predicted model and real model is $\|\mathbf{m} - \mathbf{m}_n\| < \varepsilon$ where $\varepsilon > 0$ is any small real number representing the closeness of the two model points. The closeness of the predicted and measured data can be evaluated $\|\mathbf{d} - \mathbf{d}_n\| < \delta$ $(\mathbf{d}_n = A(\mathbf{m}_n))$ when $\delta > 0$ (any small positive real number). In this way we can make the data as close as we need to the measured data, and as we do so, the predicted model $\mathbf{m}_n$ will become closer to the real model $\mathbf{m}$.

This model space may contain entries that do not fit into a correct set of solutions to our particular problem, and we therefore restrict the solution space and call this our correctness set. By using a correctness set, we can tailor our problem to run faster and to look at only valid solutions of the problem.

In the real world we find many problems that would be considered ill conditioned, and these types of problems were initially thought to be unsolvable. An ill conditioned problem is one in which two or more models produce the same data, making it impossible to determine which of the two models caused the data. In our example, for instance, for a

Y shaped branch with a break on one of the branches, we cannot tell which of the branches is broken if the two branches were originally of the same length. In a less extreme case, ambiguity or error in the measurements can cause ambiguity in the models, creating a system that is ill conditioned but may still be resolvable. If a problem is ill conditioned we can restrict the solution set to a predefined correctness set to improve the conditioning and make the solution converge to the correct model. The information to create this correctness set can be derived from a priori information such as known approximate wire lengths. A priori information is anything about the model space that is known prior to the inversion, including minimum and maximum wire lengths, configurations, allowed impedances etc.

2.3.2 Gradient Methods

The methods used in this thesis use the first derivative (the 'Frechet Derivative'), to determine the slope of the functional. This gives the fastest way to the solution (finding the model). Since the methods described in this section minimize the error between two data sets (points in our D space) by using the derivative to give us the gradient of the functional at a point, they are called "descent methods".

2.3.2.1 Descent Methods

Descent methods try to decrease the 'Misfit Functional ϕ'at each iteration using the slope of the misfit functional. [(a,b) indicates inner product, and its properties are discussed starting with equation (A.29) in the appendix.]

$$\phi = \mu_D^2 \left(A(\mathbf{m}_n), \mathbf{d}_o \right) = \mu_D^2 \left(\mathbf{d}_n, \mathbf{d}_o \right) \tag{2.1}$$

The misfit functional measures the difference between the expected data $\mathbf{d}_n$ from the actual measured data $\mathbf{d}_o$. The expected data $\mathbf{d}_n$ is computed using the forward operator $A(*)$ on the model $\mathbf{m}_n$ predicted for the current iteration n. The norm μ_D^2 of the difference between these models gives a single real number that indicates the misfit between $\mathbf{d}_n$ and $\mathbf{d}_o$. Expanding equation (2.1)

$$\begin{aligned} \phi &= \left(A(\mathbf{m}_n) - \mathbf{d}_o, A(\mathbf{m}_n) - \mathbf{d}_o \right) \\ (error)^2 &= \left(A(\mathbf{m}_n) - \mathbf{d}_o, A(\mathbf{m}_n) - \mathbf{d}_o \right) \end{aligned} \tag{2.2}$$

As the solution proceeds towards a better fit, the minimization condition [5] will be

$$\phi(\mathbf{m}_{n+1}) < \phi(\mathbf{m}_n) \quad \text{for all } n \geq 0 \tag{2.3}$$

met if the solution is converging.

The functional ϕ is aptly named the "misfit," because it is this functional (which returns a positive real number, the error squared) that determines the distance (the fit)

between the predicted data and the measured data. The $\mathbf{d}_o$ vector represents the measured TDR data. Vector $\mathbf{m}_n$ is a model parameter vector in the model space (correctness set) and can be thought of as an n-dimensional space composed of the line lengths and terminating impedances as well as the topology of the wiring network.

Using the properties of the Hilbert space the equations necessary for the method of steepest descent can be found. From the descent condition of (2.3) we take the first variation of the "misfit functional"

$$\delta_{\mathbf{m}_n}\phi(\mathbf{m}_n) = \delta_{\mathbf{m}_n}\left(A(\mathbf{m}_n)-\mathbf{d}_o, A(\mathbf{m}_n)-\mathbf{d}_o\right) \tag{2.4}$$

We will assume that $A(\mathbf{m}_n)$ is differentiable with a Taylor series expansion about $\mathbf{m}_n$ and yields $F_{\mathbf{m}}\delta\mathbf{m}$ ($F_{\mathbf{m}}$ is the Frechet derivative and $\delta\mathbf{m}$ is the variation of $\mathbf{m}$, ignoring higher order derivatives.) Since the functional (2.4) is a multiplication of two functions, the Frechet derivative may be taken using property (2.5).

$$\delta(AB) = B\ \delta A + A\ \delta B \tag{2.5}$$

Equation (2.5) is the well known derivative of the product of two functions. The derivative of the first function is multiplied by the second function and added to the

derivative of the second function times the first function.

$$\delta_{\mathbf{m}_n}\left(A(\mathbf{m}_n)-\mathbf{d}_o, A(\mathbf{m}_n)-\mathbf{d}_o\right)=\left(\delta_{\mathbf{m}_n}A(\mathbf{m}_n), A(\mathbf{m}_n)-\mathbf{d}_o\right)+\left(A(\mathbf{m}_n)-\mathbf{d}_o, \delta_{\mathbf{m}_n}A(\mathbf{m}_n)\right)$$
$$=2\left(\delta_{\mathbf{m}_n}A(\mathbf{m}_n), A(\mathbf{m}_n)-\mathbf{d}_o\right)=2\left(F_{\mathbf{m}_n}\delta\mathbf{m}_n, \mathbf{A}(\mathbf{m}_n)-\mathbf{d}_o\right) \tag{2.6}$$

Because $F_{\mathbf{m}}$ is a linear operator, its adjoint operator can be taken to the other side of equation (2.6). In our situation this adjoint operator is nothing more than the transpose of the vector $F_{\mathbf{m}}$. Thus [5]

$$2\left(F_{\mathbf{m}_n}\delta\mathbf{m}_n, \mathbf{A}(\mathbf{m}_n)-\mathbf{d}_o\right)=2\left(\delta\mathbf{m}_n, \mathbf{F}^*_{\mathbf{m}_n}\left[A(\mathbf{m}_n)-\mathbf{d}_o\right]\right) \tag{2.7}$$

I have introduced $F^*_{\mathbf{m}_n}$ here to represent the adjoint operator of the Frechet derivative.

$$F^*_{\mathbf{m}_n}=F^T_{\mathbf{m}_n} \tag{2.8}$$

To meet the start condition $\delta\mathbf{m}$ is made equal to $-k_n\mathbf{l}(\mathbf{m}_n)$, $\mathbf{l}(\mathbf{m}_n)=F^*_{\mathbf{m}_n}\left(A(\mathbf{m}_n)-\mathbf{d}_o\right)$ is the direction of steepest ascent [5]. The minimization of the input parameter vector $\mathbf{m}_n$ is found by adding $\delta\mathbf{m}$ to the previous iteration $\mathbf{m}_n$:

$$\mathbf{m}_{n+1} = \mathbf{m}_n - k_n \mathbf{l}(\mathbf{m}_n) \tag{2.9}$$

k_n is a real number called the step which controls the rate of convergence to help make sure that the method converges to the correct answer and keeps the minimization from overshooting the minimum point. The subscript indicates that k_n may be varied each time a new model parameter vector $\mathbf{m}_n$ is determined. For k_n to be selected properly the following functional is minimized:

$$\phi(\mathbf{m}_{n+1}) = \phi(\mathbf{m}_n - k_n \mathbf{l}(\mathbf{m}_n)) = \Phi(k_n) \tag{2.10}$$

The Frechet derivative is taken relative to k_n and minimized to determine the new k_n. Starting with the complete functional, recalling that $\phi = \mu_D^2(A(\mathbf{m}_n), \mathbf{d}_o)$ and substituting into (2.10) $\mathbf{m}_n$ from equation(2.9) and assuming that $k_n \mathbf{l}(\mathbf{m}_n)$ is very small, we can use a linear approximation for the forward operator $A(\mathbf{m}_n - k_n \mathbf{l}(\mathbf{m}_n)) = A(\mathbf{m}_n) - k_n F_{\mathbf{m}_n} \mathbf{l}(\mathbf{m}_n)$.

$$(A(\mathbf{m}_n - k_n \mathbf{l}(\mathbf{m}_n)) - \mathbf{d}_o, A(\mathbf{m}_n - k_n \mathbf{l}(\mathbf{m}_n) - \mathbf{d}_o)) \tag{2.11}$$

(Again, the Taylor series expansion ignores the higher order derivatives). Substituting

into equation (2.11) yields

$$\left(A(\mathbf{m}_n) - k_n F_{\mathbf{m}_n}\mathbf{l}(\mathbf{m}_n) - \mathbf{d}, A(\mathbf{m}_n) - k_n F_{\mathbf{m}_n}\mathbf{l}(\mathbf{m}_n) - \mathbf{d}\right) \tag{2.12}$$

Taking the derivative with respect to k_n.

$$-2\left(F_{\mathbf{m}_n}\mathbf{l}(\mathbf{m}_n), A(\mathbf{m}_n) - k_n F_{\mathbf{m}_n}\mathbf{l}(\mathbf{m}_n) - \mathbf{d}\right) \tag{2.13}$$

and rearranging the terms of (2.13)

$$-2\left(F_{\mathbf{m}_n}\mathbf{l}(\mathbf{m}_n), A(\mathbf{m}_n) - \mathbf{d} - k_n F_{\mathbf{m}_n}\mathbf{l}(\mathbf{m}_n)\right) \tag{2.14}$$

And expanding the inner product

$$-2\left[\left(F_{\mathbf{m}_n}\mathbf{l}(\mathbf{m}_n), A(\mathbf{m}_n) - \mathbf{d}\right) - k_n\left(F_{\mathbf{m}_n}\mathbf{l}(\mathbf{m}_n), F_{\mathbf{m}_n}\mathbf{l}(\mathbf{m}_n)\right)\right]$$

$$= -2\left[\left(\mathbf{l}(\mathbf{m}_n), F^*_{\mathbf{m}_n}\left[A(\mathbf{m}_n) - \mathbf{d}\right]\right) - k_n\left\|F_{\mathbf{m}_n}\mathbf{l}(\mathbf{m}_n)\right\|^2\right]$$

$$= -2\left[\left(\mathbf{l}(\mathbf{m}_n), \mathbf{l}(\mathbf{m}_n)\right) - k_n \left\| F_{\mathbf{m}_n} \mathbf{l}(\mathbf{m}_n) \right\|^2 \right]$$

$$= -2\left[\left\| \mathbf{l}(\mathbf{m}_n) \right\|^2 - k_n \left\| F_{\mathbf{m}_n} \mathbf{l}(\mathbf{m}_n) \right\|^2 \right] \tag{2.15}$$

Setting the result of (2.15) equal to zero, minimizes the functional to determine k_n:

$$-2\left[\left\| \mathbf{l}(\mathbf{m}_n) \right\|^2 - k_n \left\| F_{\mathbf{m}_n} \mathbf{l}(\mathbf{m}_n) \right\|^2 \right] = 0$$

$$\left\| \mathbf{l}(\mathbf{m}_n) \right\|^2 - k_n \left\| F_{\mathbf{m}_n} \mathbf{l}(\mathbf{m}_n) \right\|^2 = 0$$

$$k_n \left\| F_{\mathbf{m}_n} \mathbf{l}(\mathbf{m}_n) \right\|^2 = \left\| \mathbf{l}(\mathbf{m}_n) \right\|^2 \tag{2.16}$$

$$k_n = \frac{\left\| \mathbf{l}(\mathbf{m}_n) \right\|^2}{\left\| F_{\mathbf{m}_n} \mathbf{l}(\mathbf{m}_n) \right\|^2}$$

As the minimization of the misfit functional proceeds, the value of k_n decreases to very small numbers, thus using a reduced step size for changes to the model.

2.3.2.2 Steepest Descent Method

In every method discussed here, the first thing that is done is determination of how close the initial predicted data point $\mathbf{d}_1 = A(\mathbf{m}_1)$ (determined from our first guess of

the $\mathbf{m}_1$ model). This is accomplished by using the misfit functional. This gives the residual $\mathbf{r}_1$, which is the distance between the measured and the predicted data $\mathbf{r}_n = A(\mathbf{m}_n) - \mathbf{d}_o$. Next, the slope of the functional $\mathbf{l}_1$ at $\mathbf{m}_1$ is determined. This will tell the direction that the model parameter vector $\mathbf{m}$ must go. The general equation for the slope found at each iteration is:

$$\mathbf{l}_n = \mathbf{l}(\mathbf{m}_n) = \mathbf{F}^*_{\mathbf{m}_n} \mathbf{r}_n \tag{2.17}$$

$\mathbf{F}^*_{\mathbf{m}_n}$ is the adjoint of $\mathbf{F}_{\mathbf{m}_n}$ (adjoint of the Frechet derivative) which is only the transpose of the vector or matrix $\mathbf{F}_{\mathbf{m}_n}$ (used in the various methods of gradient minimization). This includes only the first derivative and ignores all higher order derivatives. The direction to minimize the functional is now known. The step size k_n tells how far the algorithm should proceed in the $\mathbf{l}_n$ direction. The step size (k_n) is the next thing found:

$$k_n = \frac{\|\mathbf{l}(\mathbf{m}_n)\|^2}{\|\mathbf{g}_n\|^2} \text{ where } \mathbf{g}_n = \mathbf{F}_{\mathbf{m}_n} \mathbf{l}_n \tag{2.18}$$

(Recall that the use of k_n will assure that we do not shoot over the desired result.) With

this information the next new model is found:

$$\mathbf{m}_{n+1} = \mathbf{m}_n - k_n \mathbf{l}_n \tag{2.19}$$

At every iteration the new model $\mathbf{m}_{n+1}$ is run through the forward operator $A(*)$ to find the predicted data $\mathbf{d}_{n+1}$. The residual $\mathbf{r}_{n+1}$ is calculated. When the norm of the residual $\mathbf{r}_{n+1}$ is below a predefined level ε, model $\mathbf{m}_{n+1}$ is assumed to be correct.

The modulus of the residual squared is $\phi(\mathbf{m}_n) = \|\mathbf{r}_n\|^2 \leq \varepsilon$ the program terminates when this value is below a given threshhold ε. The process is shown in Figure 2-2 with the different variables listed in (2.20).

$\mathbf{m}_n$	Wire Parameter Vector
$A(\mathbf{m}_n)$	Forword Operator - Producing TDR Data
$\mathbf{d}_o$	Measured TDR Data
$F_{\mathbf{m}_n}$	Frechet Derivative
$F^*_{\mathbf{m}_n}$	Adjoint of the Frechet Derivative
$\mathbf{r}_n$	Residual
ε	Allowed Error
$\mathbf{l}_n$	Steepest Slop at $\mathbf{m}_n$
k_n	Step
g_n	$F_{\mathbf{m}_n}\mathbf{l}_n$
$\mathbf{m}_{n+1}$	Next Wire Parameter Vector

(2.20)

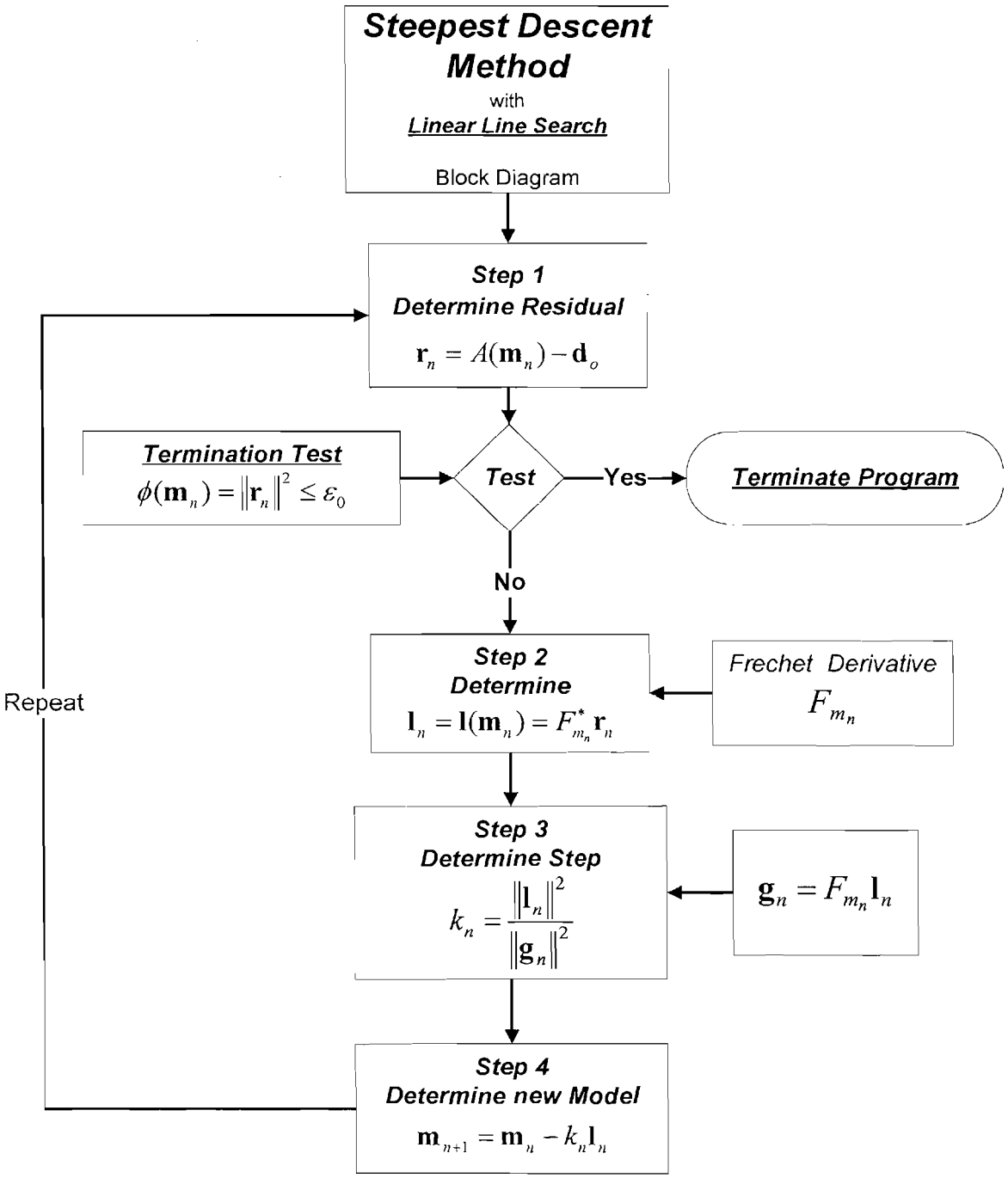

Figure 2-2 Steepest Descent Method with Linear Line Search

This process is iterative. It may take longer to converge than other methods, but it is leaner on memory usage than other methods. The memory is reused each time the derivative is taken.

2.3.2.3 Alternative Inversion Methods

2.3.2.3.1 Newton Method. The Newton method shown in Figure 2-3 differs from the steepest descent method with the idea of reducing the "misfit" in a single step. The Newton method seeks to go in one direction straight to the minimum. The starting point for this method is $\mathbf{m}_1 = \mathbf{m}_0 + \Delta\mathbf{m}$,[5]. Recall $\phi(\mathbf{m}) = \mu_D^2\left(A(\mathbf{m}), \mathbf{d}\right)$, and substitute $\mathbf{m}_1$ for $\mathbf{m}$.

$$\phi(\mathbf{m}_1) = \left(A(\mathbf{m}_0 + \Delta\mathbf{m}) - \mathbf{d}, A(\mathbf{m}_0 + \Delta\mathbf{m}) - \mathbf{d}\right) \tag{2.21}$$

Taking the Frechet derivative with respect to $\Delta\mathbf{m}$ yields

$$\delta_{\Delta\mathbf{m}}\phi(\mathbf{m}_1) = 2\left(\delta A(\mathbf{m}_0 + \Delta\mathbf{m}) - \mathbf{d}, A(\mathbf{m}_0 + \Delta\mathbf{m}) - \mathbf{d}\right) \tag{2.22}$$

An approximation for $A(\mathbf{m}_0 + \Delta\mathbf{m}) \cong A(\mathbf{m}_0) + F_{\mathbf{m}_0}\Delta\mathbf{m}$ comes from the Taylor series expansion about $\mathbf{m}_0$, ignoring the higher order terms, because $\Delta\mathbf{m}$ is small. With the

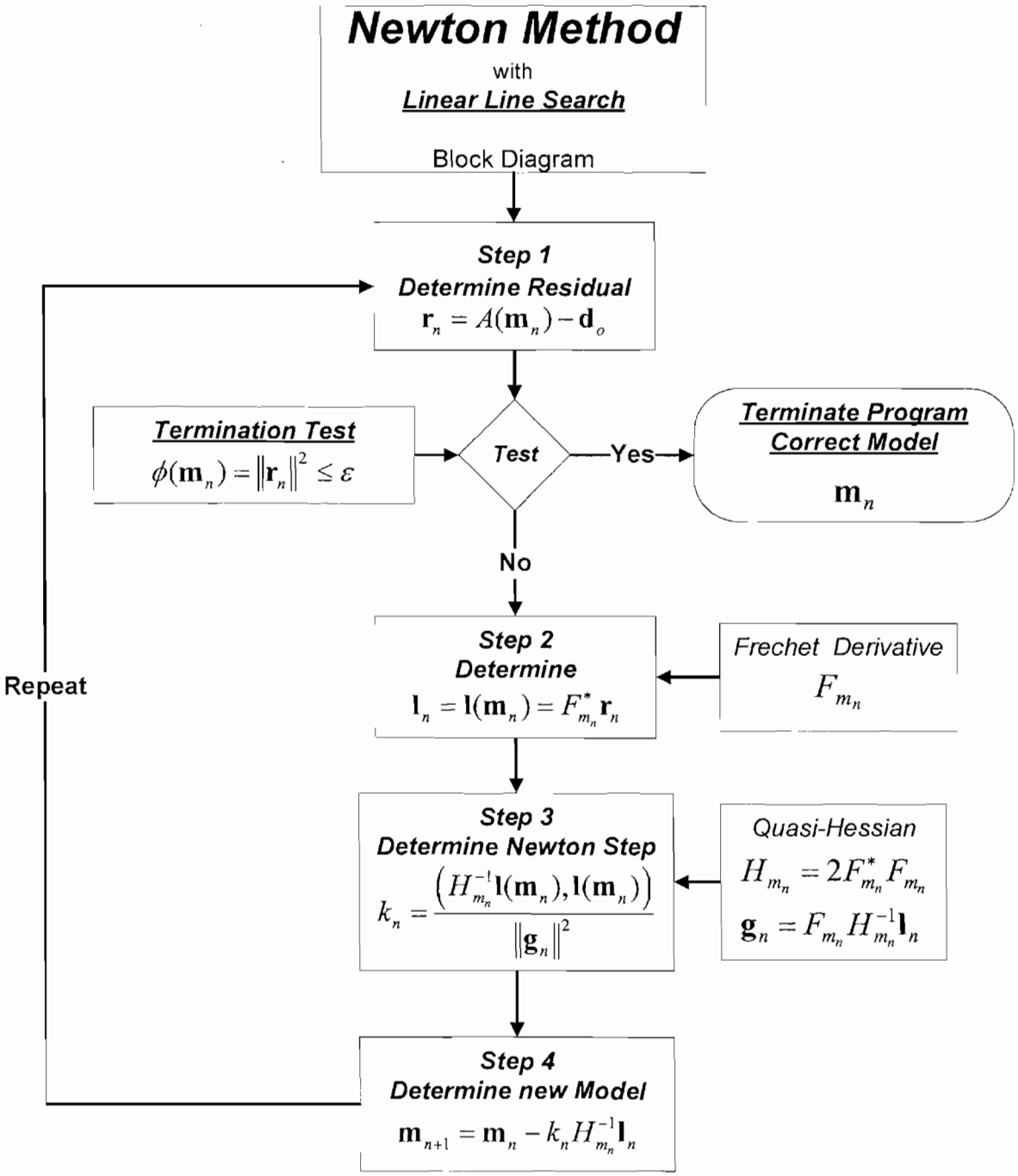

Figure 2-3 Newton Method with Linear Line Search

approximation of equation $A(\mathbf{m}_0 + \Delta\mathbf{m})$, equation (2.22) may be reduced to

$$\delta\left(A(\mathbf{m}_0) + F_{\mathbf{m}_0}\Delta\mathbf{m} - \mathbf{d}\right) = F_{\mathbf{m}_0}\delta\Delta\mathbf{m} \tag{2.23}$$

This can be simplified to:

$$\delta_{\Delta\mathbf{m}}\phi(\mathbf{m}_1) = 2\left(F_{\mathbf{m}_0}\delta\Delta\mathbf{m}, A(\mathbf{m}_0 + \Delta\mathbf{m}) - \mathbf{d}\right) \tag{2.24}$$

Using the adjoint operator, (2.24) becomes

$$\delta_{\Delta\mathbf{m}}\phi(\mathbf{m}_1) = 2\left(\delta\Delta\mathbf{m}, F^*_{\mathbf{m}_0}\left(A(\mathbf{m}_0 + \Delta\mathbf{m}) - \mathbf{d}\right)\right) \tag{2.25}$$

Using the same notion as before and approximating $A(\mathbf{m}_0 + \Delta\mathbf{m})$ by $A(\mathbf{m}_0) + F_{\mathbf{m}_0}\Delta\mathbf{m}$ and substituting this into equation (2.25), it is found that

$$\delta_{\Delta\mathbf{m}}\phi(\mathbf{m}_1) = 2\left(\delta\Delta\mathbf{m}, F^*_{\mathbf{m}_0}\left(A(\mathbf{m}_0) + F_{\mathbf{m}_0}\Delta\mathbf{m} - \mathbf{d}\right)\right) \tag{2.26}$$

This is the first variation of the functional. Think of this as the derivative of a function;

at its minimum the slope of the derivative goes to zero. Everything surrounding the minimum is at a greater magnitude than at the minimum. If it is a true minimum the function will start heading back up from the minimum. At the minimum, the slope is equal to zero [5], so set equation (2.26) equal to zero.

$$\delta_{\Delta \mathbf{m}}\phi(\mathbf{m}_1) = 2\left(\delta\Delta\mathbf{m}, F_{\mathbf{m}}^{*}\left(A(\mathbf{m}_0) + F_{\mathbf{m}}\Delta\mathbf{m} - \mathbf{d}\right)\right) = 0 \tag{2.27}$$

Equation (2.27) should always be equal to zero regardless of the value of $\delta\Delta\mathbf{m}$, and therefore

$$F_{\mathbf{m}_0}^{*}\left(A(\mathbf{m}_0) + F_{\mathbf{m}_0}\Delta\mathbf{m} - \mathbf{d}\right) = 0 \tag{2.28}$$

Because $F_{\mathbf{m}_0}^{*}$ is a linear operator $F_{\mathbf{m}_0}^{*}$ can be taken within the brackets, yielding

$$F_{\mathbf{m}_0}^{*}\left[A(\mathbf{m}_0) - \mathbf{d}\right] + F_{\mathbf{m}_0}^{*}F_{\mathbf{m}_0}\Delta\mathbf{m} = 0$$

$$F_{\mathbf{m}_0}^{*}F_{\mathbf{m}_0}\Delta\mathbf{m} = -F_{\mathbf{m}_0}^{*}\left[A(\mathbf{m}_0) - \mathbf{d}\right] \tag{2.29}$$

$$F_{\mathbf{m}_0}^{*}\left[A(\mathbf{m}_0) - \mathbf{d}\right] = \mathbf{l}(\mathbf{m}_0)$$

$$F_{\mathbf{m}_0}^{*} F_{\mathbf{m}_0} \Delta\mathbf{m} = -\mathbf{l}(\mathbf{m}_0)$$

$$H_{\mathbf{m}_0} = 2F_{\mathbf{m}_0}^{*} F_{\mathbf{m}_0} \tag{2.30}$$

$$\frac{1}{2} H_{\mathbf{m}_0} \Delta\mathbf{m} = -\mathbf{l}(\mathbf{m}_0)$$

From (2.30) the change $\Delta\mathbf{m}$ can be found

$$\Delta\mathbf{m} = -2H_{\mathbf{m}_0}^{-1}\mathbf{l}(\mathbf{m}_0) \tag{2.31}$$

From $\Delta\mathbf{m}_0$, $\mathbf{m}_1$ can be found

$$\mathbf{m}_1 = \mathbf{m}_0 - 2H_{\mathbf{m}_0}^{-1}\mathbf{l}(\mathbf{m}_0) \tag{2.32}$$

given that the inverse of $H_{\mathbf{m}_0}$ exists. The Newton method will converge in one iteration for a linear operator $A(\bullet)$ but requires more iterations for a nonlinear operator. Equation (2.32) is modified to allow for multiple iterations

$$\mathbf{m}_{n+1} = \mathbf{m}_n - k_n H_{\mathbf{m}_n}^{-1}\mathbf{l}(\mathbf{m}_n) \tag{2.33}$$

The step k_n is usually used to help the method converge for nonlinear operators. The Newton method with line search algorithm finds the step by using $\phi(\mathbf{m}_{n+1})$ and taking its first variation with regard to k_n and then minimizing it to find the smallest step:

$$\phi(\mathbf{m}_{n+1}) = \phi\left(\mathbf{m}_n - k_n H_{\mathbf{m}_n}^{-1}\mathbf{l}_n\right)$$

$$\delta_{k_n}\phi(\mathbf{m}_{n+1}) = \delta_{k_n}\left(A\left(\mathbf{m}_n - k_n H_{\mathbf{m}_n}^{-1}\mathbf{l}_n\right) - \mathbf{d}, A\left(\mathbf{m}_n - k_n H_{\mathbf{m}_n}^{-1}\mathbf{l}_n\right) - \mathbf{d}\right) \tag{2.34}$$

If it is assumed that $k_n H_{\mathbf{m}_n}^{-1}\mathbf{l}_n$ is small, a linear approximation can be applied to $A\left(\mathbf{m}_n - k_n H_{\mathbf{m}_n}^{-1}\mathbf{l}_n\right)$ giving the approximation of $A(\mathbf{m}_n) - k_n F_{\mathbf{m}_n} H_{\mathbf{m}_n}^{-1}\mathbf{l}_n$. Substituting into equation (2.34) gives

$$\begin{aligned}&\delta_{k_n}\left(A(\mathbf{m}_n) - k_n F_{\mathbf{m}_n} H_{\mathbf{m}_n}^{-1}\mathbf{l}_n - \mathbf{d}, A(\mathbf{m}_n) - k_n F_{\mathbf{m}_n} H_{\mathbf{m}_n}^{-1}\mathbf{l}_n - \mathbf{d}\right)\\ &\quad = -2\left(F_{\mathbf{m}_n} H_{\mathbf{m}_n}^{-1}\mathbf{l}_n, A(\mathbf{m}_n) - \mathbf{d} - k_n F_{\mathbf{m}_n} H_{\mathbf{m}_n}^{-1}\mathbf{l}_n\right)\end{aligned} \tag{2.35}$$

Setting (2.35) to zero

$$-2\left(F_{\mathbf{m}_n}H_{\mathbf{m}_n}^{-1}\mathbf{l}_n, A(\mathbf{m}_n)-\mathbf{d}-k_nF_{\mathbf{m}_n}H_{\mathbf{m}_n}^{-1}\mathbf{l}_n\right)=0$$

$$\left(F_{\mathbf{m}_n}H_{\mathbf{m}_n}^{-1}\mathbf{l}_n, A(\mathbf{m}_n)-\mathbf{d}-k_nF_{\mathbf{m}_n}H_{\mathbf{m}_n}^{-1}\mathbf{l}_n\right)=0 \tag{2.36}$$

And reducing equation (2.36) allows us to find the step k_n

$$\left(H_{\mathbf{m}_n}^{-1}\mathbf{l}_n, F_{\mathbf{m}_n}^{*}\left[A(\mathbf{m}_n)-\mathbf{d}\right]\right)-k_n\left(F_{\mathbf{m}_n}H_{\mathbf{m}_n}^{-1}\mathbf{l}_n, F_{\mathbf{m}_n}H_{\mathbf{m}_n}^{-1}\mathbf{l}_n\right)=0$$

$$\left(F_{\mathbf{m}_n}H_{\mathbf{m}_n}^{-1}\mathbf{l}_n, A(\mathbf{m}_n)-\mathbf{d}\right)-\left(F_{\mathbf{m}_n}H_{\mathbf{m}_n}^{-1}\mathbf{l}_n, k_nF_{\mathbf{m}_n}H_{\mathbf{m}_n}^{-1}\mathbf{l}_n\right)=0$$

$$k_n\left(F_{\mathbf{m}_n}H_{\mathbf{m}_n}^{-1}\mathbf{l}_n, F_{\mathbf{m}_n}H_{\mathbf{m}_n}^{-1}\mathbf{l}_n\right)=\left(H_{\mathbf{m}_n}^{-1}\mathbf{l}_n, F_{\mathbf{m}_n}^{*}\left[A(\mathbf{m}_n)-\mathbf{d}\right]\right) \tag{2.37}$$

$$k_n=\frac{\left(H_{\mathbf{m}_n}^{-1}\mathbf{l}_n, F_{\mathbf{m}_n}^{*}\left[A(\mathbf{m}_n)-\mathbf{d}\right]\right)}{\left(F_{\mathbf{m}_n}H_{\mathbf{m}_n}^{-1}\mathbf{l}_n, F_{\mathbf{m}_n}H_{\mathbf{m}_n}^{-1}\mathbf{l}_n\right)}$$

Recall that $F_{\mathbf{m}_n}^{*}\left[A(\mathbf{m}_n)-\mathbf{d}\right]$ is $\mathbf{l}_{m_n}$ and that

$$\left(F_{\mathbf{m}_n}H_{\mathbf{m}_n}^{-1}\mathbf{l}_n, F_{\mathbf{m}_n}H_{\mathbf{m}_n}^{-1}\mathbf{l}_n\right)=\left\|F_{\mathbf{m}_n}H_{\mathbf{m}_n}^{-1}\mathbf{l}_n\right\|^2 \tag{2.38}$$

Substituting these back into equation (2.37) gives k_n : [5 p135]

$$k_n = \frac{\left(H_{\mathbf{m}_n}^{-1}\mathbf{l}_n, \mathbf{l}_n\right)}{\left\|F_{\mathbf{m}_n} H_{\mathbf{m}_n}^{-1}\mathbf{l}_n\right\|^2} \tag{2.39}$$

The Newton method algorithm is as follows: in order to find the direction to the minimum, the Newton method takes the derivative of the all the parameters in the network model at the point of the initial $\mathbf{m}_n$. These derivatives are placed in a matrix called $\mathbf{F}_{\mathbf{m}}$. The Frechet derivative is then multiplied by its adjoint to give a quasi-Hessian[5] operator:

$$H_{\mathbf{m}_n} = 2\mathbf{F}_{\mathbf{m}_n}^{*}\mathbf{F}_{\mathbf{m}_n} \tag{2.40}$$

It is referred to as quasi-Hessian, because it does not use the 2nd Frechet derivative and is therefore a linear operator. If the inverse of this quasi-Hessian matrix exists, $\Delta\mathbf{m}$ can be found:

$$\begin{aligned} \Delta\mathbf{m} &= -k_n H_{\mathbf{m}_n}^{-1}\mathbf{l}\left(\mathbf{m}_n\right) \\ \mathbf{m}_{n+1} &= \mathbf{m}_n - k_n H_{\mathbf{m}_n}^{-1}\mathbf{l}\left(\mathbf{m}_n\right) \end{aligned} \tag{2.41}$$

Multiple iterations are usually needed to converge to the correct answer for a nonlinear

operator.

Upon entering the algorithm the residual is found first, determining the closeness of the initial data vector $\mathbf{d}_1$ and the measured data $\mathbf{d}_o$. Next the Frechet derivative $\mathbf{F}_{m_n}$ is found for each parameter in the wire network (model) vector $\mathbf{m}_n$. Next the slope $\mathbf{l}_n$ is determined by multiplying the Frechet derivative $\mathbf{F}_{m_n}$ by the residual $\mathbf{r}_n$. Next the semi-Hessian operator is found using equation (2.40). Then the step size k_n is determined from (2.39) and $\mathbf{m}_{n+1}$ from equation (2.41). We continue through this process shown in Figure 2-3 returning to the beginning of the algorithm and repeating the steps. The error (misfit) is determined again, and when the misfit is minimized, i.e., $\phi(\mathbf{m}_n) = \|\mathbf{r}_n\|^2 \leq \varepsilon$, the program is terminated.

2.3.2.3.2 Conjugate Gradient Method. The conjugate gradient method shown in Figure 2-4 takes a shorter path to the minimum than does the steepest decent method. The idea is that each time the descent changes directions and takes the conjugate direction from the previous direction, thus allowing for faster convergence to the correct answer than steepest descent. The method bypasses local minima as well, due to converging to an answer on multiple levels. The basic equations used, are found.[5] The same techniques for finding the necessary equations for the method are used, with simplifying assumptions extended to the nonlinear operator case from the linear case. β_n is derived in Zhdanov's book on pages 138 to 141. [5] The equations are basically those equations that were used in the steepest descent method with additions for the conjugate

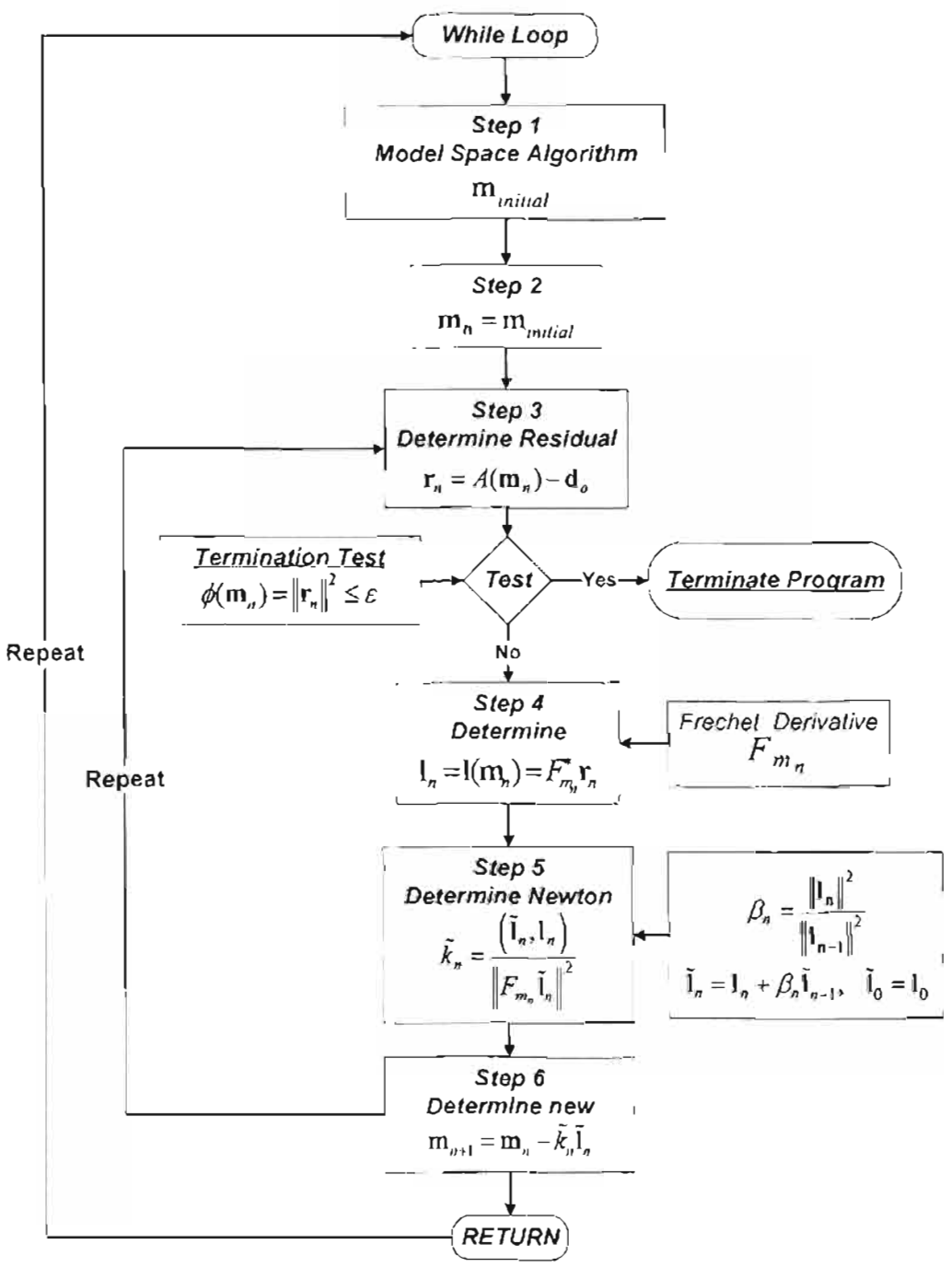

Figure 2-4 Conjugate Gradient Method with Linear Line Search

direction. The residual is

$$\mathbf{r}_n = A(m_n) - \mathbf{d} \tag{2.42}$$

The slope of the misfit at $\mathbf{m}_n$ is

$$\mathbf{l}_n = \mathbf{l}(\mathbf{m}_n) = F^*_{m_n}\mathbf{r}_n \tag{2.43}$$

From what has already been found, β_n can be evaluated. Using β_n times the previous direction and adding this value to the steepest descent slope gives the direction followed next and assures that the direction is conjugate to the direction that was followed previously:

$$\beta_n = \frac{\|\mathbf{l}_n\|^2}{\|\mathbf{l}_{n-1}\|^2} \tag{2.44}$$

$$\tilde{\mathbf{l}}_n = \mathbf{l}_n + \beta_n \tilde{\mathbf{l}}_{n-1}, \quad \tilde{\mathbf{l}}_0 = \mathbf{l}_0 \tag{2.45}$$

This method also uses a linear line search k_n.

$$\tilde{k}_n = \frac{\left(\tilde{\mathbf{l}}_n, \mathbf{l}_n\right)}{\left\| F_{\mathbf{m}_n} \tilde{\mathbf{l}}_n \right\|^2} \tag{2.46}$$

When all the information is calculated, the next model vector is found:

$$\mathbf{m}_{n+1} = \mathbf{m}_n - \tilde{k}_n \tilde{\mathbf{l}}_n \tag{2.47}$$

This process also terminates when the error is below a given threshold ε

$$\phi\left(\mathbf{m}_{\mathrm{n}}\right) = \left\|\mathbf{r}_{\mathrm{n}}\right\|^2 \leq \varepsilon \tag{2.48}$$

To reduce the possibility of error, the algorithm in this thesis will use initial (a priori) information to make a well conditioned problem (make the problem solvable) and reduce the number of possible mappings of the network being sought. Doing this should speed convergence.

2.3.2.4 Model Space

Figure 2-5 shows the way the model parameter vector for the wiring network is created and what each number in the model vector $\mathbf{m}$ represents. These model

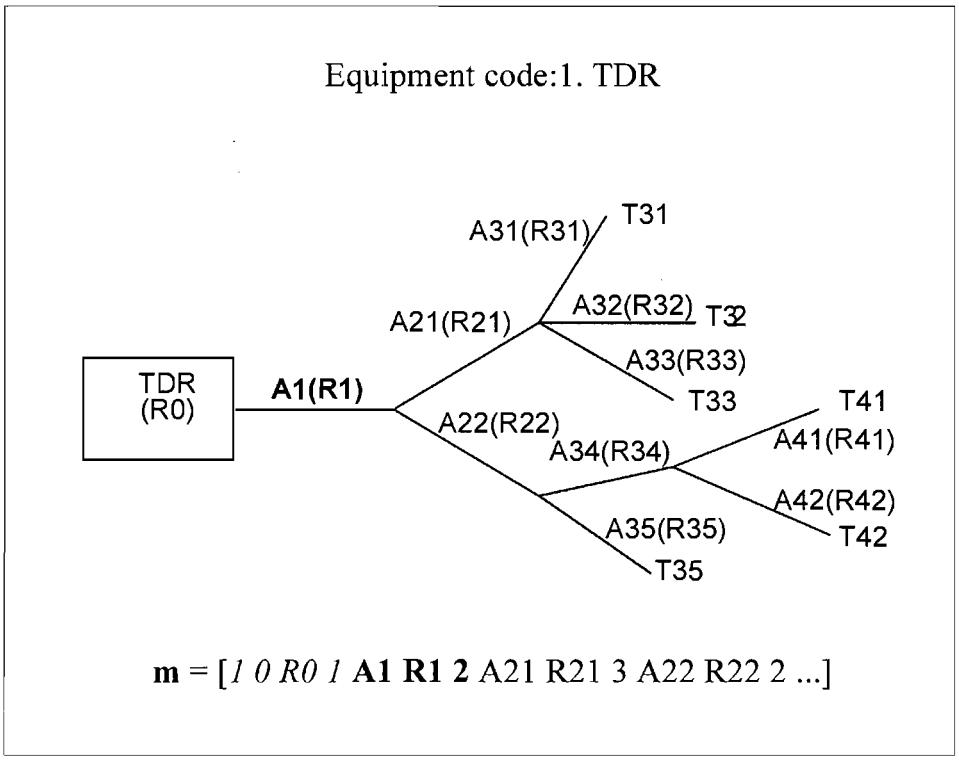

Figure 2-5 Model Space

parameters change depending on the configuration of the network. After the first four parameters of the **m** vector (which represent the configuration of the forward operator to generate TDR data), the parameters representing each wire come in groups of three. The first group of three is highlighted in red in the figure. The first of the three parameters is the length of the wire in meters ($A1$). The next parameter $R1$ is the characteristic impedance of the wire in ohms. The third parameter is the number of wires that connect to the end of this wire (an integer limited to 3 for our application, based on a priori

knowledge about typical aircraft wiring topologies).

The general idea is to take the proposed model vector $\mathbf{m}$ of the predicted network and run it through the forward operator, producing a predicted TDR response. This predict $\mathbf{d}_n$ response is compared to the measured response $\mathbf{d}_o$ of the wiring network to determine the misfit functional. This will be explained in much more detail later.

The misfit functional takes the two vectors of data ($\mathbf{d}_n$ and $\mathbf{d}_o$, the predicted and measured TDR responses) and finds out how close they are to each other. It does this by subtracting the measured data $\mathbf{d}_o$ from the calculated data $\mathbf{d}_n$ from the most recent iteration of the model $\mathbf{m}_n$. It then takes the inner product (2.2) of the difference with itself, which yields the squared distance between the two data sets. Taking the square root of this yields the error or misfit. Using variational calculus, the slope of the misfit functional is determined. Following this slope with a step size of k_n provides the quickest way to minimize the functional.

There are many methods of applying steepest descent that minimize the misfit functional. Each method has a starting assumption that determines how the minimization is to be performed. The new model parameter $\mathbf{m}_{n+1}$ is the next iteration of the predicted model given the previous model $\mathbf{m}_n$. n is the n^{th} iteration through the algorithm. With the length and direction of the next step $\delta\mathbf{m}$ can again be found. The step is added to the previous model's parameters $\mathbf{m}_n$ to give $\mathbf{m}_{n+1}$, where $\mathbf{m}_{n+1} = \mathbf{m}_n + \delta\mathbf{m}_n$. When the misfit is reduced to a preset threshold, the program terminates.

2.3.2.5 Frechet Derivative

This section describes the "Frechet Derivative" in some detail and the errors that can be introduced by taking differences between data that may lie close to each other. The Frechet derivative is the partial derivative of the forward operator evaluated at $\mathbf{m}_n$ with respect to each parameter of the model vector $\mathbf{m}_n$. The Frechet derivative is determined numerically either by taking the central difference or by taking the forward or backward difference of the forward operator $A(\mathbf{m}_n)$ [6].

Figure 2-6 illustrates the central difference method for determining the differential. Each element (m_i) of the parameter vector $\mathbf{m}_n$ is taken one by one and varied by some amount $\delta m_i / 2$, and then this difference is divided by $\|\delta m_i\|$.

$$A(\mathbf{m}+\frac{\delta \mathbf{m}_i}{2}), A(\mathbf{m}-\frac{\delta \mathbf{m}_i}{2}) \tag{2.49}$$

$$F_{m_i} = \frac{A(\mathbf{m}+\frac{\delta \mathbf{m}_i}{2}) - A(\mathbf{m}-\frac{\delta \mathbf{m}_i}{2})}{\|\delta \mathbf{m}_i\|} \tag{2.50}$$

This process is done for each element of the network parameter vector and stored in $F_{\mathbf{m}_n}$. The steepest descent method computes the derivative of one element of the network parameter vector at a time, whereas in the Newton and conjugate gradient

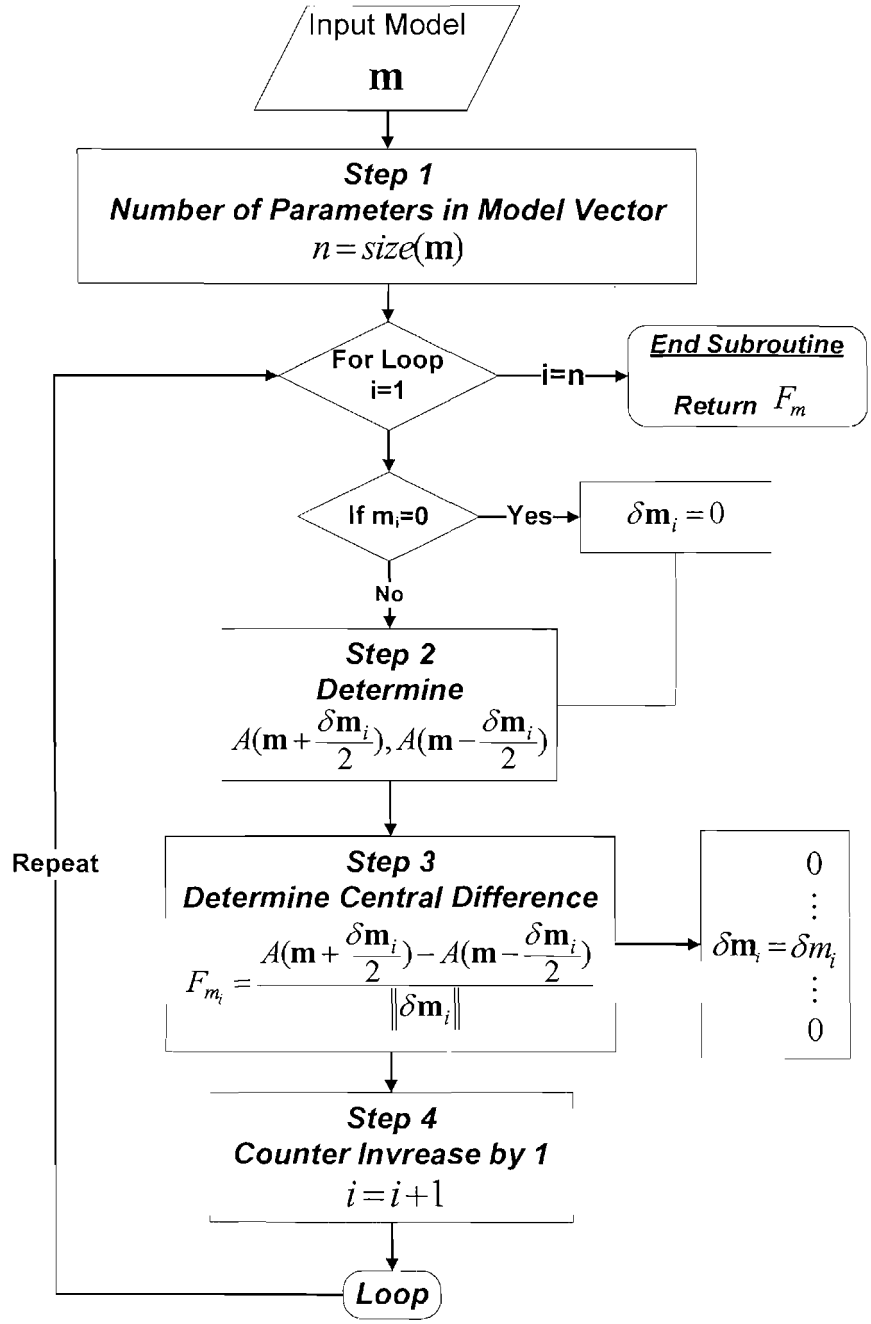

Figure 2-6 Frechet Derivative

methods the partial derivatives of each of the elements of the network parameter vector are evaluated every time the Frechet derivative is taken.

Because each parameter of the model **m** vector is varied by different amounts in performing the derivative, the algorithm determines the amount of this variation of the parameter contained in the vector each time the derivative is evaluated at $\mathbf{m}_n$. The process continues until all of the parameters in the **m** vector have been minimized. If the model parameter is equal to zero, it is skipped to make sure that the termination's length parameter is not changed. Changing the length parameter of a termination would change the topology of the network.

The Newton and conjugate gradient methods require that all parameters of the current model be evaluated due to their minimization of the misfit functional on multiple levels. The steepest descent method is somewhat easier to follow than the other two methods that have been discussed.

2.3.2.5.1 Errors. Because the Frechet derivative requires taking the difference equation (2.50), of two closely spaced functions, a numerical error may be introduced that could cause the computed derivative to diverge from the actual derivative. If the forward operator is fairly benign, the spacing between input parameters can be moved further apart, and the difference can then be taken with little error being introduced into the problem.

Two types of error that we should address.[7]

- Round Off Error: The error introduced by representing a real number as a

floating point number used on a computer is round off error. This kind of error can be minimized by using extended precision. Any real number can be represented to any precision we desire, i.e. the number 2 can be represented exactly, and π can be represented to any precision, but when we try to represent it on a computer we are limited by the number of digits that are available. Some numbers can be represented exactly, such as 2 in a base 2 system, but other numbers are either rounded up or down to the nearest floating point number that can be represented by the computer. This round off introduces error.

- Truncation Error: Truncation error has no rounding involved. Instead digits are truncated after a certain precision (number of digits) has been reached. The effects of round off and truncation error are very similar.

2.3.2.6 Inner Product

The inner product is the integral of the product of two operands of the function. Shown here in integral form

$$\left(f(x),g(x)\right)=\int_a^b f(x)g(x)dx \tag{2.51}$$

This inner product is classified as an L_2 inner product. The norm with this inner product

in this Hilbert space is

$$\left\|\left(f(x)\right)\right\| = \sqrt{\int_a^b f(x) f(x)\, dx} \tag{2.52}$$

The (referring to Figure 2-7) way that this is performed numerically is that each element of one vector is multiplied be the elements of the other vector. Each element is then summed up, simulating the integral of the two vectors.

2.4 Summary

The methods of steepest descent (Steepest Descent, Newton, and Conjugate Gradient) have been derived and explained with the use of the misfit functional and simplifying assumptions. The Frechet derivative was introduced and used throughout the derivation of the methods. In order to make the problem solvable a correctness set was introduced that defined what the allowed answers would look like. Various types of numerical errors were described.

The next chapter describes in detail the specific problem this thesis is solving. More definition is given of the model space and how a model parameter vector is created. Insights into the TDR data are brought out to help in understanding how the problem of finding the wiring map was solved.

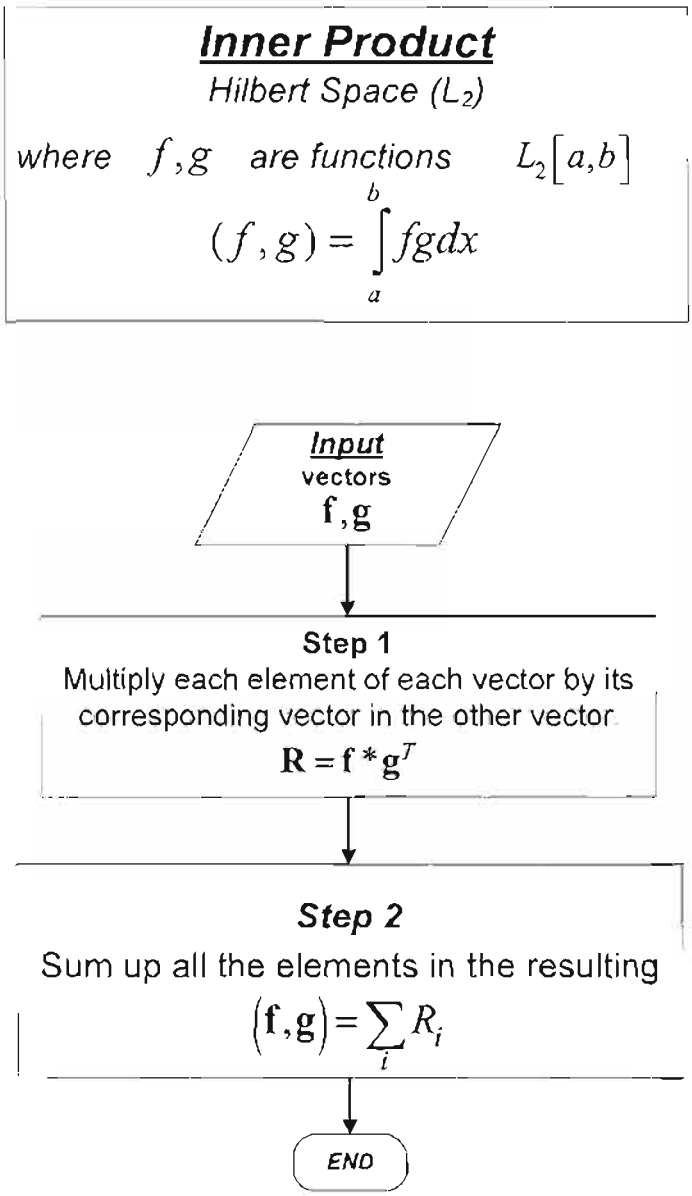

Figure 2-7 Inner Product

CHAPTER 3

METHOD: STEEPEST DESCENT

The data $\mathbf{d}_o$ for this application have been measured using a Time Domain Reflectometer, and the topology of the wire structure that caused the response is the desired output. The method of solving the inverse problem will now be discussed. Chapter 2 described three methods of minimization: Steepest descent, Newton, and conjugate gradient. All three methods where tested and compared for the determination of the model. Because of its simplicity, the steepest descent method was used to minimize the misfit functional one parameter at a time, which helped in understanding what was happening with the problem of finding the wire network map.

In this section each component of the problem will be described.

3.1 Forward Operator

The forward operator is needed to create simulated TDR data $\mathbf{d}_n$ from the wire network model parameter vector $\mathbf{m}_n$. The simulated TDR data are then compared with the measured TDR data. The forward operator program written by Dr. Lo [8] uses a matrix based calculation approach. This was performed by subdividing the input wire

network into equal length segments. This allowed the network to be modeled as a matrix where each segment is modeled by an entry in this matrix as either the transmission coefficient through the particular segment or the reflection coefficient at its end.

With the use of a state vector $\bar{\mathbf{x}}_{t-1}$ and the matrix representing the network, the TDR response of the network can be calculated using the following equation

$$\bar{\mathbf{x}}_t = \mathbf{A}\bar{\mathbf{x}}_{t-T} \tag{3.1}$$

Equation (3.1) shows that by multiplication of the network matrix with the state vector $\mathbf{x}_{t-T}$ a new state vector is generated that represents the state of the network at the next slice in time.

3.1.1 More on the Model Parameter Vector

The forward operator program requires a vector input representing the proposed wire network. This operator can produce a map of the wiring network along with the TDR response data $\mathbf{d}_n$. The model $\mathbf{m}$ of our operator $A(\mathbf{m})$ is a vector with multiple parameters, each parameter causing the Forward Operator to output data in some predefined way. The branched wire model space is shown in Figure 3-1.

The model vector $\mathbf{m}$ uses the first four parameters to represent the measuring system, in general $\begin{bmatrix} i_1 & r_2 & r_3 & i_4 & \cdots \end{bmatrix}$. "$i$" is used to represent an integer, and a "r" is used

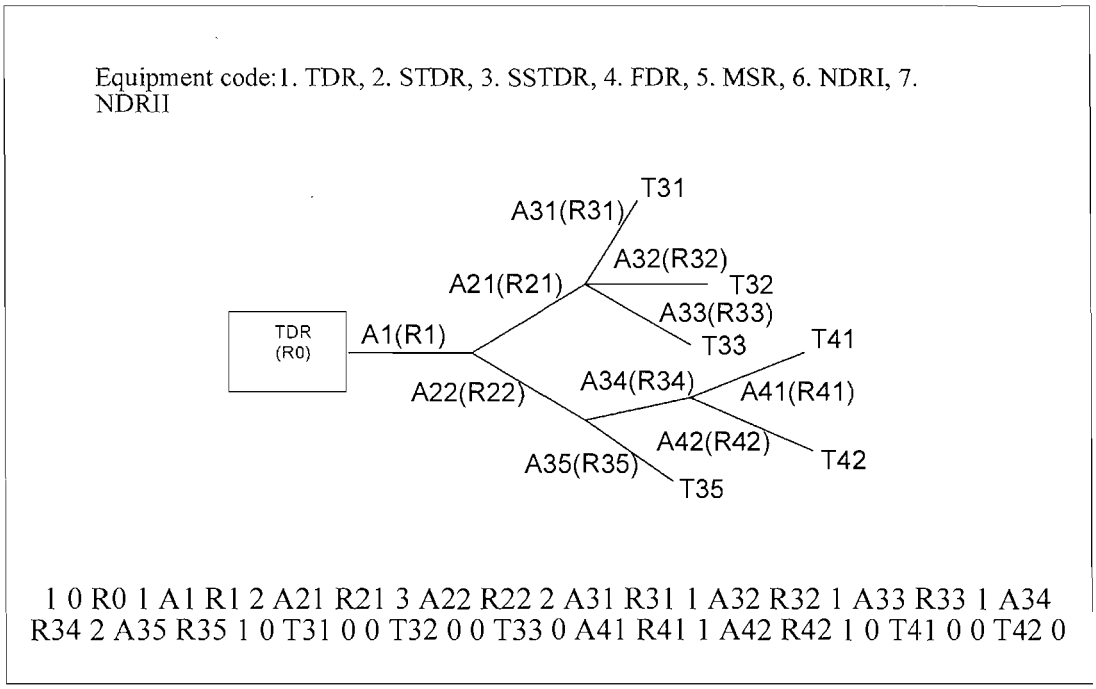

Figure 3-1 Model Space for a Large Branched Network Model

to represent a positive real number. The subscripts represent the position of the number within the vector. The first of the four numbers i_1 represents the type of data that will be generated by the forward operator. A list of equipment types that can be generated by this forwardoperator are found below. The focus for this thesis is on the TDR type data; therefore $i_1 = 1$. All other types of data can be used instead, so this is just a choice, not a requirement.

1. TDR – Time Domain Reflectometry
2. STDR – Sequence Time Domain Reflectometry
3. SSTDR – Spread Spectrum Time Domain Reflectometry

4. FDR – Frequency Domain Reflectometry
5. MSR – Mixed Signal Reflectometry

The next of the four numbers r_2 represents the length of the central cable used with the testing equipment and is not considered to be part of the wiring network. The third number r_3 represents the impedance of the measuring device (50Ω is used for TDR driver). The final number in the first four model parameters i_4 represents the number of follow on connecting wires, which for this thesis has been held to one.

If we remove the first four parameters from the vector $\mathbf{m}$, the remaining parameters can be parsed into groups of three. Each group of three has A R #W. In Figure 3-1, A1 R1 2 are the first group of three, A21 R21 3 are the second group of three, and so on, continuing through to the end of the model vector.

Each group of three parameters has the following pattern:

- A indicates the length of the transmission line in meters. This number is a real number.
- R indicates the characteristic impedance of the transmission line in ohms. This is a real number.
- #W represents the number of wires connected to the wire of length A. This must be a positive integer $0 \le n \le 3$ (0 represents a termination, 1 represents one wire, 2 represents a "y" shaped network, "3" is a single wire connecting to 3 others).

Terminations have zero length and are only placed at the end of single wires.

- An open circuit is represented as"0 999 0" indicating a wire of zero length, an

impedance of 999 (in the forward operator the impedance of 999 means an open) with no follow on connections.

- A short circuit is represented as "0 0 0" which again means zero length, the impedance of the line equal to zero, with no follow on connecting wires .

It is helpful to think (Referring to Figure 3-2) of these wires being placed on different levels when referring to the wire network parameter. The third number in each group of three indicates how many wires are at the next level. An example of the preceding discussion is illustrated by an example of a wiring network parameter vector. The **m** vector is broken down into a first group of four, and then the rest of the parameters are broken down into groups of three as has already been explained. The levels of each section are brought out by the numbering of each item and Figure 3-2 shows the levels in block diagram form.

Example: (refer to Figure 3-2)

$$\mathbf{m} = [1\ 0\ 50\ 1\ 20\ 50\ 2\ 30\ 75\ 1\ 45\ 50\ 1\ 0\ 999\ 0\ 0\ 0\ 0]$$

1) Decoding the model vector into parameters

   a. First four parameters

      i. 1 0 50 1 would decode as a TDR measurement with zero length wire connection and a 50Ω system impedance and one connecting wire.

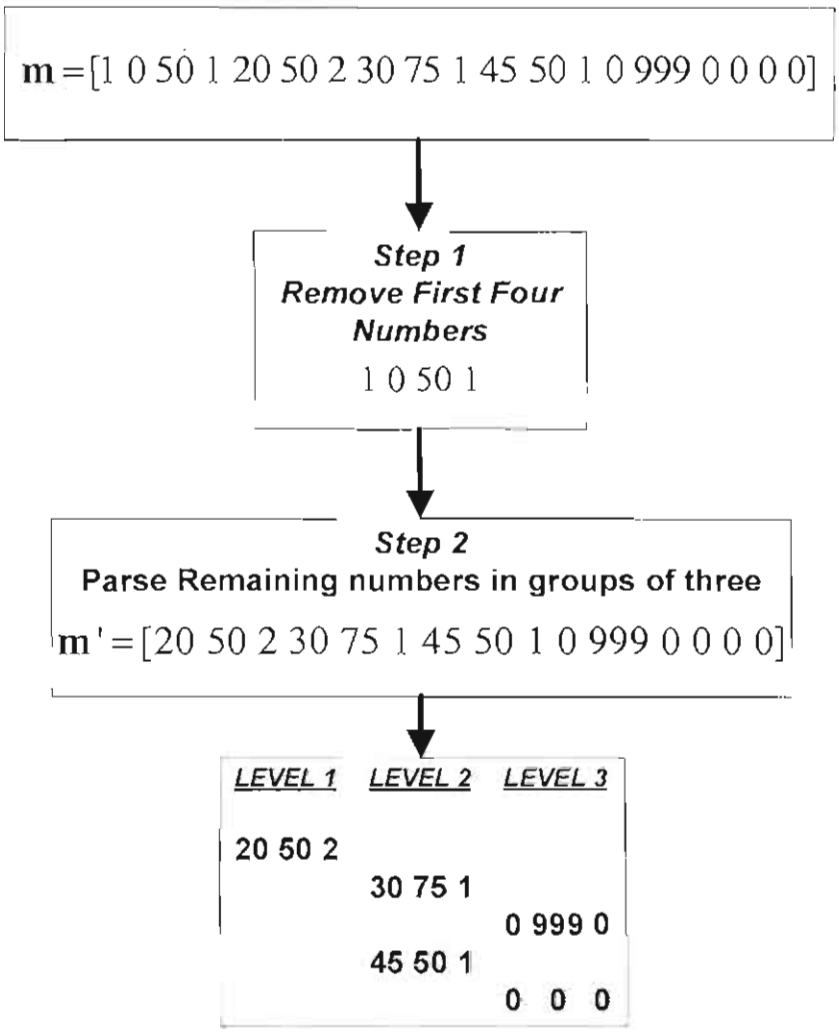

Figure 3-2 Model Parameter Vector

2) Removing the first four parameters leaving

$$\mathbf{m}' = [20\ 50\ 2\ 30\ 75\ 1\ 45\ 50\ 1\ 0\ 999\ 0\ 0\ 0\ 0] \tag{3.2}$$

3) Sectioning into groups of three

a. 20 50 2 (level 1)

Length = 20 meters, transmission line impedance = 50Ω and two follow on connecting wires, so we will find two wires at the next level (Level 2).

i. 30 75 1 (level 2)

Length = 30 meters, transmission line impedance = 75Ω with 1 follow on connecting wire at the next level 3.

1. 0 999 0 (level 3)

Terminating the wire is an open circuit, zero length and an impedance of 999 with zero follow on connections.

ii. 45 50 1 (second wire of level 2)

Length = 45 meters, Transmission Line Impedance = 50Ω with one follow on connecting wire.

1. 0 0 0 (level 3)

A short circuit termination zero length and an impedance of zero ohms with zero follow on connections.

This completes the forward model definition.

The bottom portion of Figure 3-3 is an example of the output of the forward operator given the wiring network in the upper portion of Figure 3-3. The data are marked off in distance and not in time, and the plot (Figure 3-3, bottom) shows the discontinuities where wires and terminations meet in the wiring network. The distance between these discontinuities is determined by how far away the discontinuity is from the measuring equipment.

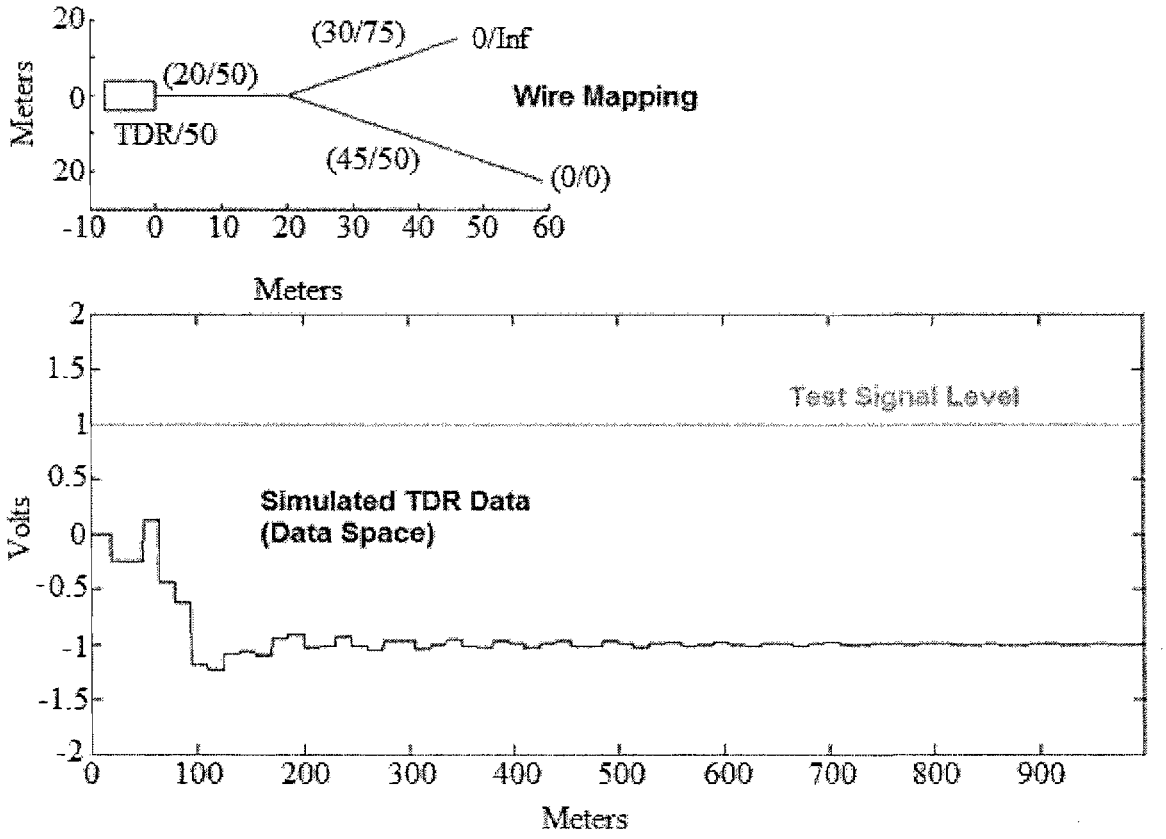

Figure 3-3 Simulated Output Data from the Forward Operator

An expanded view of Figure 3-3 is shown in Figure 3-4. The first wire has a length of 20m and as can be seen at point A in Figure 3-4, because the first reflection occurs at 20m. The next reflection occurs at the length of the first wire 20m plus the length of the shortest of the two connecting wire 30m. Therefore at 50m (point B) of the same figure there would be another reflection and then the longest of the two connecting wires is next with 45m plus the length of the first wire 20m again yielding another reflection at 65m (point C of Figure 3-4).

3.1.2 Insights

3.1.2.1 Insight 1: TDR Equipment Measures only Reflections

Because the impedance of the first wire is 50Ω, and the impedance of the TDR

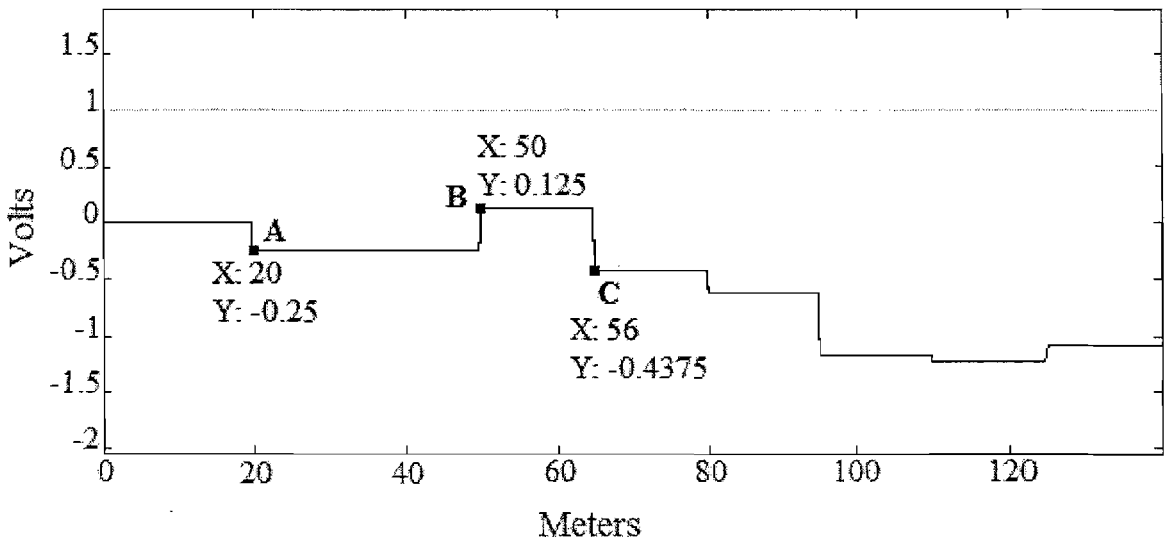

Figure 3-4 Expanded Data Space from Figure 3-3

measurement equipment is the same, the reflection at the input to the network is equal to 0. There is no reflection at this input, because an impedance discontinuity does not exist.

Figure 3-5 is what can be called a reflection and transmission map. It shows the initial (first time) reflections and transmissions at discontinuities into and out of the wiring network.

3.1.2.2 Insight 2: The First Wire's Characteristic Impedance Is Seen in the First Reflection from the Wiring Network

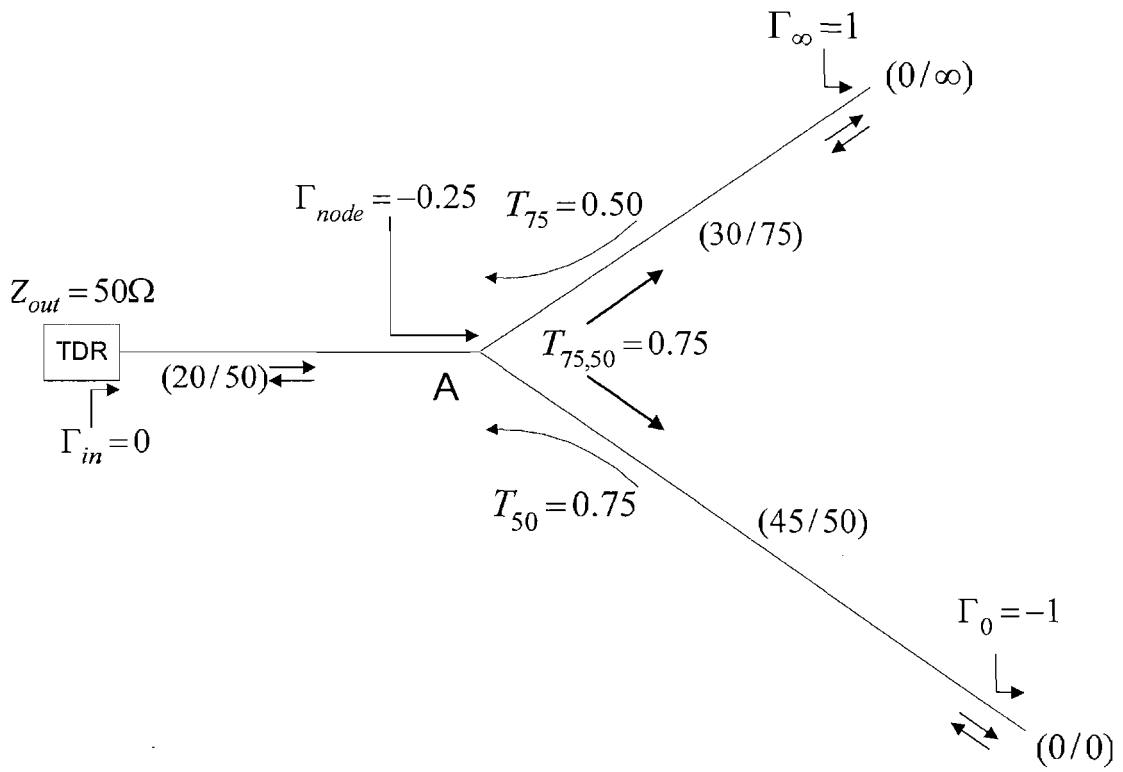

Figure 3-5 Reflection Map

In this case the reflection coefficient being equal to zero tells us that the transmission line's characteristic impedance is the same as that of the impedance of the measuring equipment which is 50Ω.

The next impedance change is found at the node where two wires are connected to the first wire, as seen in Figure 3-5 at point A. The impedance at this point, as seen from the left of point A looking to the right of Point A, is a 75Ω wire in parallel with a 50Ω wire $(75\Omega//50\Omega = 30\Omega)$ which yields an impedance of 30Ω, with a reflection coefficient of

$$\Gamma_B = \frac{30-50}{30+50} = -0.25 \tag{3.3}$$

As can be seen in Figure 3-4 the resulting voltage seen at the input to the network is $0V + (-)0.25V = -0.25V$ at point A. Every TDR reflection back to the input of the wiring network is summed with what was previously measured. For other methods, the reflections may look like pulses rather than steps.

3.1.2.3 Insight 3: Indication of the Level of Discontinuity

At point B (Figure 3-4), just after the voltage discontinuity, is the sum of the first reflection (zero in this case) with the next reflection (-0.25V) the level of this discontinuity in TDR data is the reflected wave and is an indication of the transmission

lines' parallel impedances.

If the reflection coefficient was a 1or a -1, we would have known that the line was terminated with an open or a short circuit, respectively. If the reflection is less than this, we would be able to tell if it has been terminated with another transmission line. If the reflection coefficient is small enough, it would be possible to determine if the line was terminated with more than one transmission line.

The transmitted signal that passes to the parallel combination of the 75Ωwire and to the 50Ω wire is $1V - 0.25V = 0.75V$. This could also be found using the transmission coefficient T shown in equation (3.4)

$$T = \frac{2(Z_L)}{Z_s + Z_L} \tag{3.4}$$

In our case we have

$$T = \frac{2(30)}{50 + 30} = \frac{60}{80} = 0.75 \tag{3.5}$$

yielding $1V * 0.75 = 0.75V$ which is what was there was determined previously. The same voltage is on both wires traveling to the end of each wire to their own terminations.

At the ends of the two wires there is an open circuit terminating the 75Ω wire and

a short circuit terminating the 50Ω wire. The reflection coefficients of each cable are

$$\Gamma_{open} = \frac{\infty - 75}{\infty + 75} = 1$$
$$\Gamma_{short} = \frac{0 - 50}{0 + 50} = -1 \tag{3.6}$$

When the signal is reflected back toward the input of the wire network, occurring at the wire's termination, the signal again sees an impedance discontinuity at the node point A connecting the first wire with the two wires as shown in Figure 3-5. The impedance is now seen looking from the right of node A from each of the two different wires looking into the node at point A from the right of the node. The impedance at node A will be different for each of the two wires to the right of the node. The impedance from the 75Ω line looking into node A would be two 50Ω lines in parallel.

$$50\Omega // 50\Omega = \frac{50(50)}{50 + 50} = 25\Omega \tag{3.7}$$

The impedance looking from the remaining 50Ω line terminated with the short would be the 75Ω wire in parallel with the 50Ω line, $75\Omega // 50\Omega = 30\Omega$.

Because the impedances seen by each of the terminated wires are different, secondary reflections are set up between point A and the terminations of the two wires.

Because each terminated wire sees a different impedance looking into point A the amount of reflection will be different on each line. Transmission coefficients will also be different.

First the 75Ω cable sees two 50Ω cables in parallel (for a total of 25Ω) yielding a transmission coefficient of

$$T_{75} = \frac{2(25)}{25+75} = 0.5 \tag{3.8}$$

If we were to follow the signal from the TDR equipment down through the wiring network we would see the following voltages: $1V$ sent down the network, and at node A there would be a reflection of -0.25V back to the input and measured at the TDR sensor. The transmitted signal through node A would be $0.75V$ towards the open circuit termination. At the open circuit all of the signal would be reflected back toward node A. At node A we would see a transmission coefficient of

$$\frac{2(25)}{75+25} = \frac{50}{100} = 0.50 \tag{3.9}$$

The reflected wave of $0.75V$ would reach node A of Figure 3-5 and transmit through the node with a transmission of 0.50 of the $0.75V$, yielding $0.375V$ and at the TDR

equipment sensor and would be added to $-0.25V$ giving the sum of $0.125V$, which is the voltage just past point B of Figure 3-4. This takes care of the initial reflections going to the termination of the 75Ω wire. The next reflection would be that coming from the remaining 50Ωwire with a short for a termination. Starting at node A we have $0.75V$ traveling down the 50Ωwire and reflecting at the short circuit (Figure 3-5). This is totally reflected back to node A at $-0.75V$ and at node A it is transmitted through the node with a transmission coefficient of

$$\frac{2(30)}{50+30}=\frac{60}{80}=0.75 \tag{3.10}$$

yielding $0.75V*(-0.75)=-.5625V$. Adding this to the voltage already seen by the sensor ($0.125V$) equals $-0.4375V$ which is the level to right of point C Figure 3-4.

All the initial reflections from the network have now been found and computed. From Figure 3-3 we can see that there are numerous secondary reflections that become progressively smaller as the wave reflects and transmits within the system.

3.1.2.4 Insight 4: We Do Not Need All of the Input TDR Data

Determination of the total network does not require all the data that are given by the forward operator. The information that we need is generally within the initial reflections of the wiring network.

3.1.2.5 Insight 5: The Lengths of the Wires are found in the Location of the Discontinuities of the Given Data

The higher order reflections will be taken out one by one as the primary reflections are found and removed via the residual. The focus needs to be on the initial reflections from the wiring network.

3.2 Frechet Derivative

The steepest descent method requires the use of partial derivatives (central differences) of the misfit functional with respect to each of the parameters of the model vector $\mathbf{m}_n$ in order to find the mapping of the wiring network.

$$A(\mathbf{m}+\frac{\delta\mathbf{m}_i}{2}), A(\mathbf{m}-\frac{\delta\mathbf{m}_i}{2}) \tag{3.11}$$

$$F_{m_i} = \frac{A(\mathbf{m}+\frac{\delta\mathbf{m}_i}{2}) - A(\mathbf{m}-\frac{\delta\mathbf{m}_i}{2})}{\|\delta\mathbf{m}_i\|} \tag{3.12}$$

3.3 Functional Space

It is illustrative to see what the misfit functional looks like as a function of various parameters of the model space. If we restrict the number of parameters to two we can generate three-dimensional diagrams of the misfit functional. This will also show if the

misfit functional space is benign and if the first derivative will be all that is needed to minimize the misfit functional. It will also inform us as to whether it would be practical to lengthen out the magnitude of the variation $\|\delta \mathbf{m}_i\|$ in the $\mathbf{m}_i$ elements of the parameter vector $\mathbf{m}$, so that the difference equations will be of good accuracy.

In Figure 3-6 the two parameters that are allowed to vary are the transmission line characteristic impedance and the line termination. Holding the line length constant in Figure 3-6 and allowing the characteristic impedance and the terminating impedance to vary shows how the misfit functional space appears. From the figure Z_o is equal to 500Ω and the terminating impedance Z_L is equal to 500Ω. Also seen from Figure 3-6 is the nature of the misfit functional. Note that in this case there is only one global minimum. Some misfit functionals may have more than one global minimum. The next three plots show another transmission line with the transmission line length and the line impedance as the variables that are allowed to vary across the parameter space. The plotting of the misfit also illustrates the geometry that is achieved through the misfit functional and makes clear the idea that this surface can have slope. As can be seen from all the plots there is one minimum for a single wire with a single termination. This may not be the case for more complex wiring networks.

Additional plots (Referring to Figure 3-7, Figure 3-8, Figure 3-9) were made by taking slices out of the misfit functional space so that they could be examined more closely. One parameter was allowed to vary at a time.

Figure 3-10 shows that the terminating impedance of 999Ω is more like an open

circuit than the real impedance of 999Ω, because of how this was designed into the forward operator. This can be seen in the way that the misfit shows an abrupt change in its value at 999Ω. What

Figure 3-10 shows is that if the derivative is taken at a termination of 999Ω the slope would be wrong, so finding the derivative at 999Ω should be avoided and this termination should be considered to be the open circuit.

With the terminating impedance changed to 300Ω in Figure 3-11 it can be seen that the nature of arrival at the minimum is substantially different from the case shown in Figure 3-10. The 999Ω point shows an abrupt change when it is reached as in Figure 3-10.

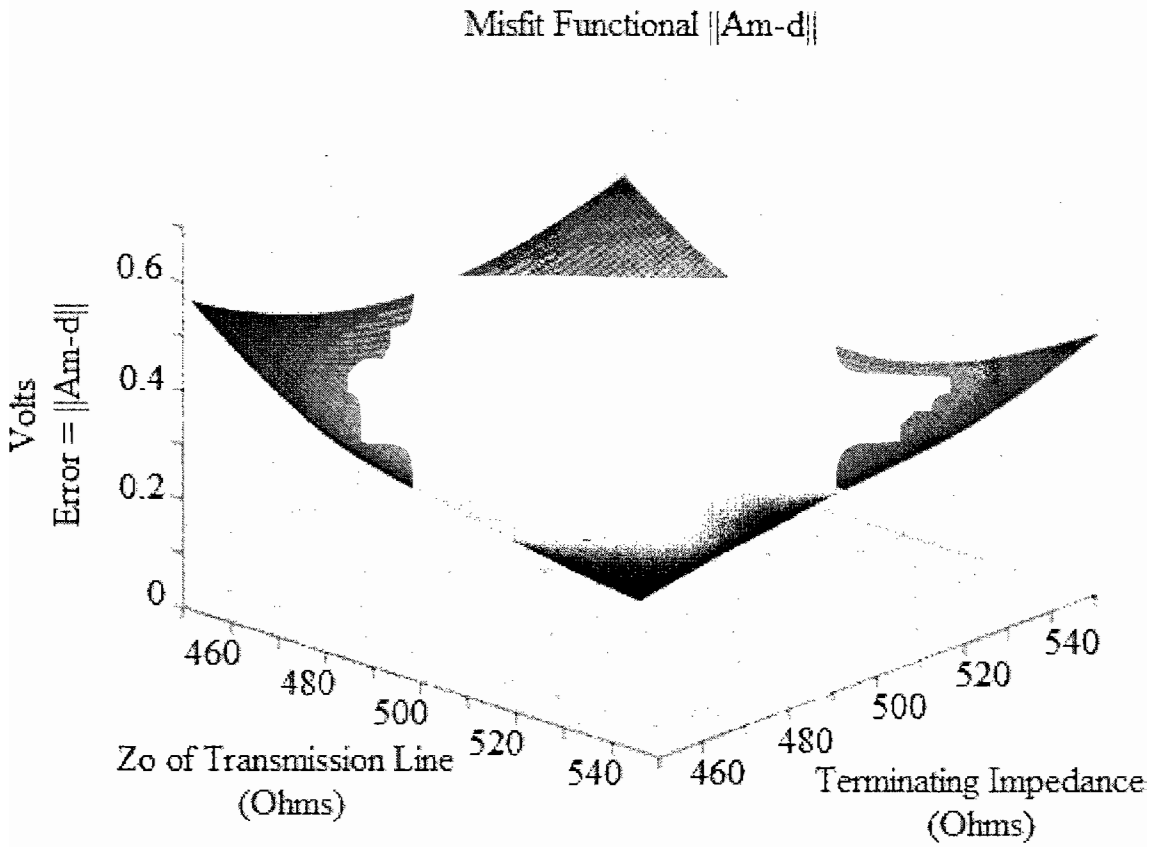

Figure 3-6 Misfit Function Space Impedance Allowed To Vary

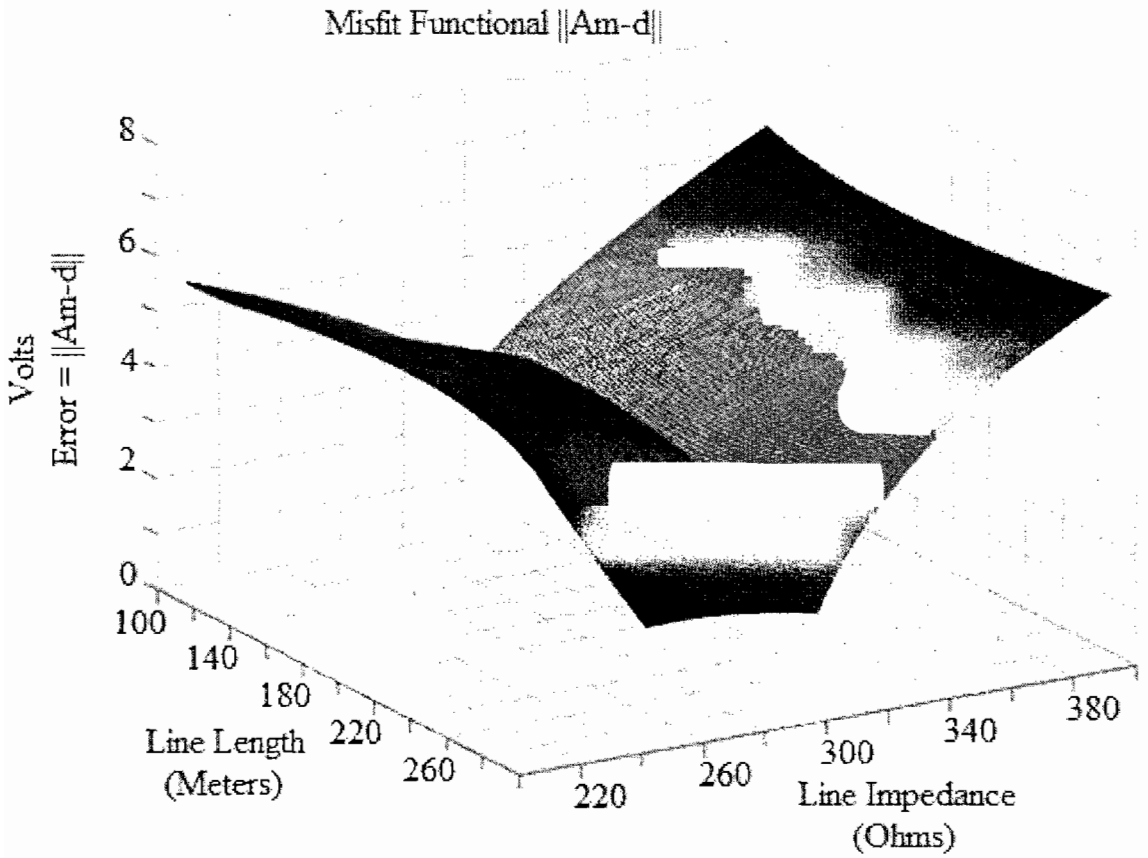

Figure 3-7 Misfit with Length and Line Impedance Varied

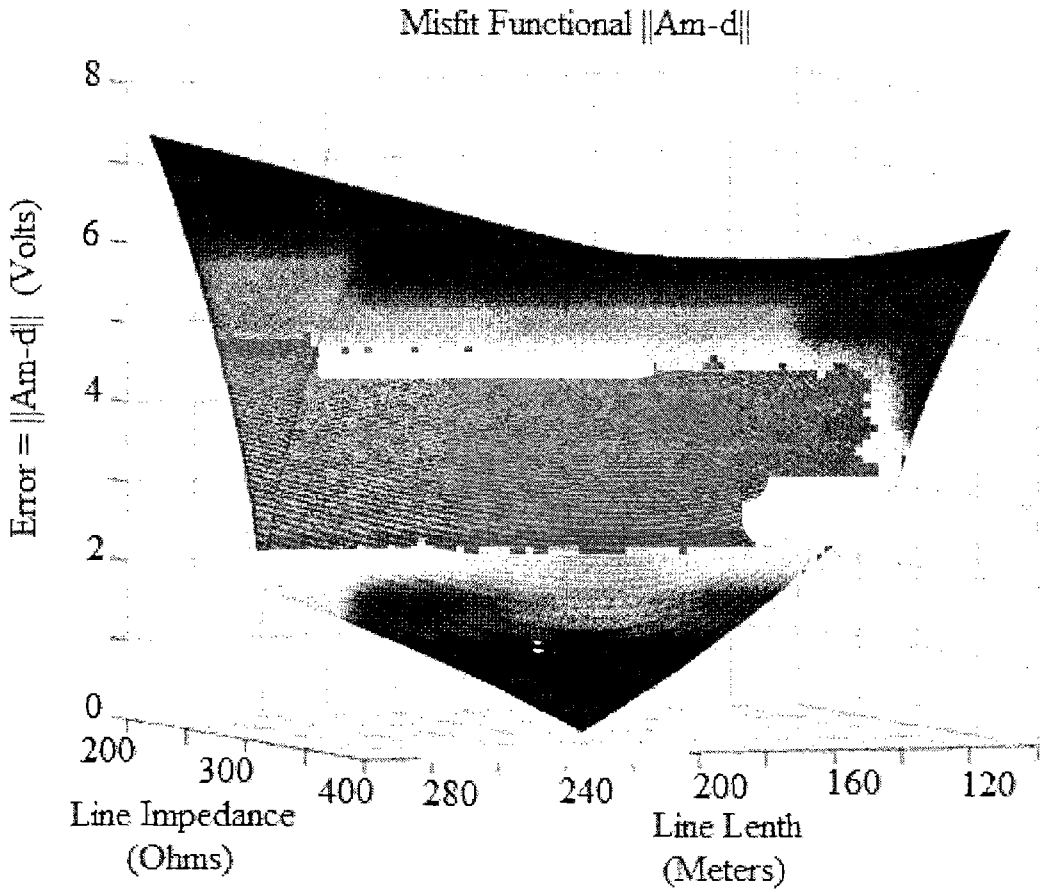

Figure 3-8 Misfit From Figure 3-7 Viewed From A Different Angle

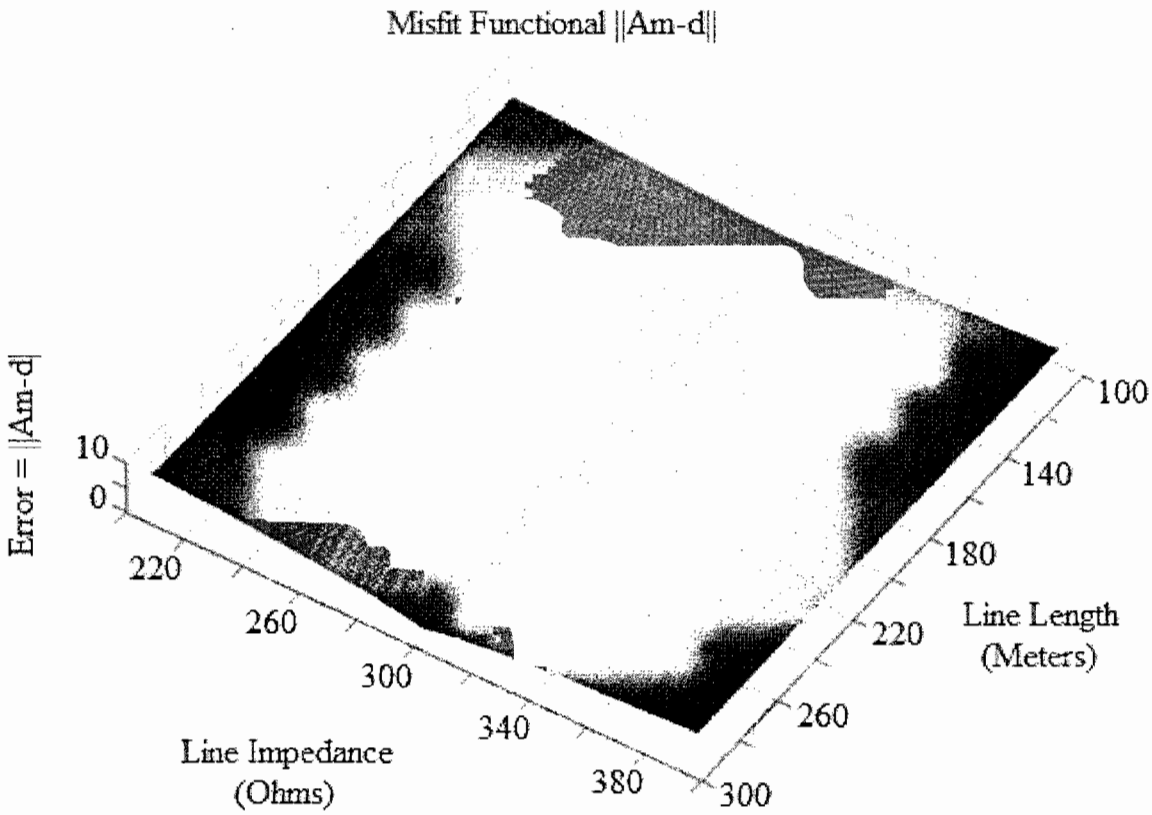

Figure 3-9 Misfit Functional Viewed From Above

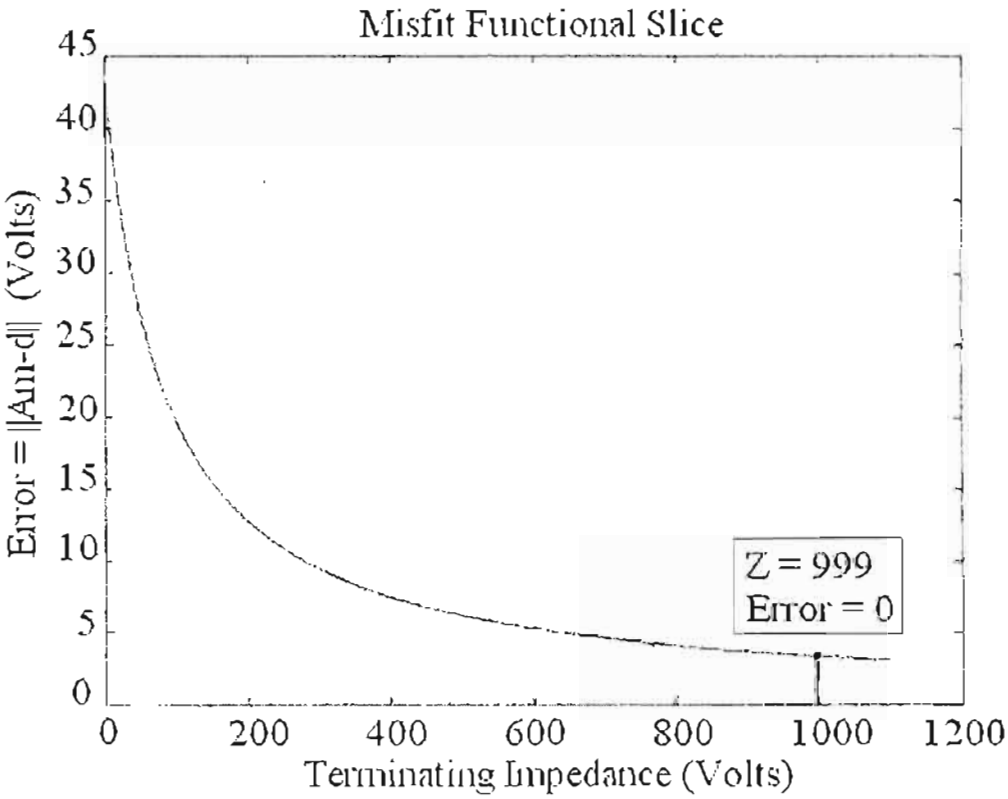

Figure 3-10 Impedance Variation - Open Circuit

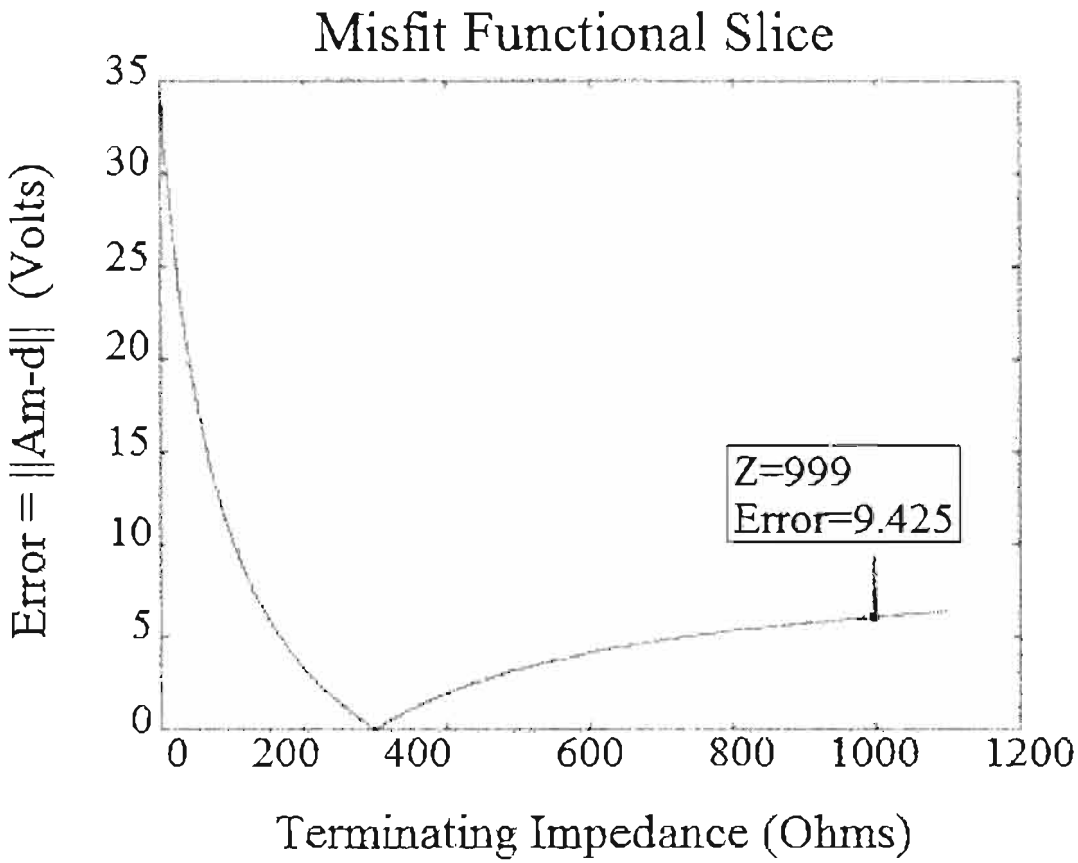

Figure 3-11 Smooth Transition To Misfit Function Minimum

CHAPTER 4

RESULTS

The previous chapter discussed methods of minimization of steepest descent. The method of steepest descent was chosen because of its simplicity, since we only need to find intermediate impedance discontinuities.

4.1 Correctness Set

The characteristic impedance, Z_o, will be of the following impedance values $50\Omega, 75\Omega, 125\Omega, 200\Omega - 300\Omega$ (where $Z_o/3$ will range from 48Ω to 54Ω).

The limiting structure of the network is shown in Figure 2-1.

These impedance values and structure restrict the solution set so that reasonable answers to the wire mapping can be found.

4.2 A Priori Information

Much a priori information is imbedded in the TDR data and can easily be extracted. Some of this information would not need to be found through iterative methods and would allow a more efficient method of finding the wire network.

4.2.1 First Wire (Connected to the TDR equipment)

The type of information that could be extracted from the data would include initial reflection coefficients and distance information between impedance discontinuities i.e., those found in the first wire connected to the TDR measuring equipment. The first reflection at the TDR measuring equipment would tell the impedance of the wire itself, because the TDR equipment's output impedance is specified by the manufacturer. For the TDR used in this thesis, the output impedance is 50Ω.

4.2.2 Length of Transmission Lines

An important realization about TDR data is that they are a record of reflections back to the source of the wiring network with each reflection recorded over time 3.1.2.1. With the time and speed of the test signal into and through the network with different reflections being recorded as functions of time, the distance to impedance discontinuities can be determined and cataloged. The distance between primary reflections tells the length of the transmission lines (3.1.2.5).

4.2.2.1 Reverberations

Reverberations (multiple reflections) can occur between impedance discontinuities, and these are also recorded by the TDR probe. Reverberations have a muddying effect on the TDR data, because the impedance discontinuities' locations would be intermingled with the reverberations. These reverberations can be removed at intermediate steps from the data via the residual equation (4.1).

$$\mathbf{d}_o - A(\mathbf{m}_n) \tag{4.1}$$

This form (4.1)of the residual is a modified version from that previously explained and is used to preserve the polarity of the data $\mathbf{d}_o$.

As each wire is found a model vector is generated and described as the $\mathbf{m}_n$ vector. This model vector is mapped into the TDR data space through the forward operator producing the reflections that would be generated by this newly found wiring network, with all of its main reflections and secondary reflections (reverberations). These reflections are removed from the input TDR data via the residual (equation (4.1)), allowing the next impedance discontinuity to be determined.

4.2.3 Reflection Polarity

Reflections can cause polarity changes based on the relative nature of the impedances seen at the discontinuity. The reflection coefficient (4.2)shows that if $Z_1 > Z_2$, Γ is a positive quantity, and if $Z_1 < Z_2$, Γ is a negative quantity with $\|\Gamma\|$ being the same in both cases.

$$\Gamma = \frac{Z_1 - Z_2}{Z_1 + Z_2} \tag{4.2}$$

The direction of travel into these impedance discontinuities makes a difference in the

polarity of the reflection but not in the magnitude of the reflection at the discontinuity.

4.2.3.1 Transmission Coefficients

An important note is that the transmission coefficient shows no such polarity change. Equation (4.3) below shows the transmission coefficient coming from Z_1 into Z_2. There is no change in phase. The same can be said of coming

$$\frac{2Z_2}{Z_1+Z_2} \tag{4.3}$$

from the opposite direction from Z_2 to Z_1 where the transmission coefficient would be $2Z_1/(Z_1+Z_2)$. Because of this lack of polarity change of the transmission coefficient the phase of a reflection from a termination is always preserved, allowing a direct indication of the type of termination (open or short circuit). To illustrate this, refer to Figure 4-1, which shows only transmission coefficients, ignoring reflections at point B of Figure 4-1.

The test signal goes through impedance discontinuities at points A and B. This test signal is reduced in amplitude by the transmission through these impedance discontinuities (A and B). At point B (Figure 4-1) the voltage wave splits into two waves, each traveling down one of two wires that are terminated at C or at D. Each voltage wave has the same voltage level at the start point B.

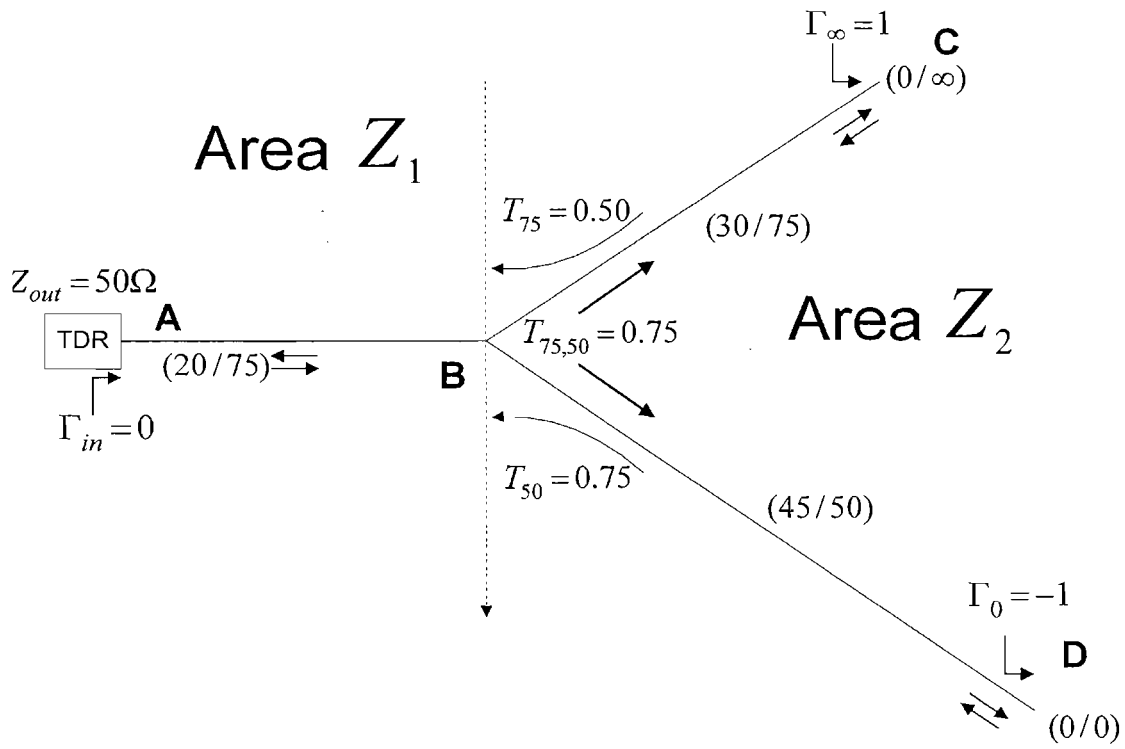

Figure 4-1 Transmission Through the Wiring Network

Consider the wave traveling down wire C (termination) only. At termination C the voltage wave is reflected back towards point B. The voltage wave will transmit through point B and down through point A into the recording device for the TDR measurement. The polarity of the termination is preserved in the transmission of the voltage wave through the wiring network all the from the terminating load and back to the source, thus giving an idea of the type of termination (open or short). This allows a test for the type of termination based on the polarity of the return. An open would have a positive polarity, and a short would have a negative polarity.

Because of other reflections from previous impedance discontinuities these terminating reflections may be hidden. We should recall that the return voltage is the sum of all reflections. The TDR response shows these returns in a step like manner as the reflections are recorded over time. The reflection from any discontinuity is recorded in the difference in the voltage level between preceding or succeeding steps, and this voltage level would also be a product of any propagation through impedance discontinuities.

By taking the derivative of the TDR input data we can find the impulse response which gives a direct indication of the location and the level of the return signal from terminations and other discontinuities (impedance) in the wiring network. The impulse response is used in the sections that follow.

4.2.4 Recovery of Main Reflections and Their Locations

Figure 4-2 shows that reverberations (reflections) would occur between node A and node B as well as between node C and B and nodes D and B. These reverberations would occur while the test signal travels to the termination of each wire. These reverberations have a muddying effect and would have to be stripped away from the TDR data in order to extract the impedance discontinuities from the TDR data.

This is precisely what is done in this thesis to recover the location of the impedance discontinuities from the TDR information

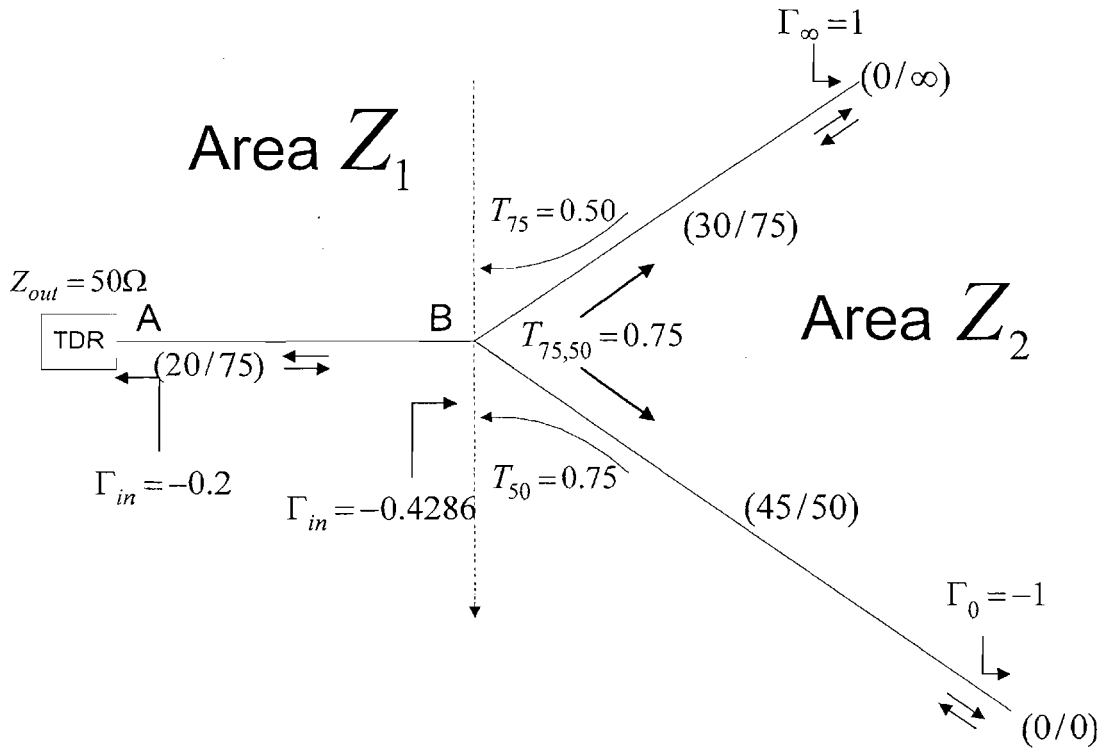

Figure 4-2 Reflections and Transmissions

4.3 Testing Algorithm - Generate TDR Data (Simulated TDR Data)

The starting point is the generation of the TDR data using the forward operator as described in section 3.1.1. The parameter vector used for the generation of the data is

$$\begin{aligned}\mathbf{m}=&[1\ 40\ 75\ 2\ 50\ 75\ 3\ 44\ 75\ 3\ 23\ 150\ 1\ 43\ 150\ 1\ 63\ 150\ 1\ 35\ 159\\ &1\ 30\ 159\ 1\ 45\ 159\ 1\ 0\ 0\ 0\ 0\ 999\ 0\ 0\ 0\ 0\ 0\ 999\ 0\ 0\ 0\ 0\ 0\ 999\ 0]\end{aligned} \tag{4.4}$$

The wiring network is mapped out in Figure 4-3. The figure shows that there are six terminations consisting of open and short circuits.

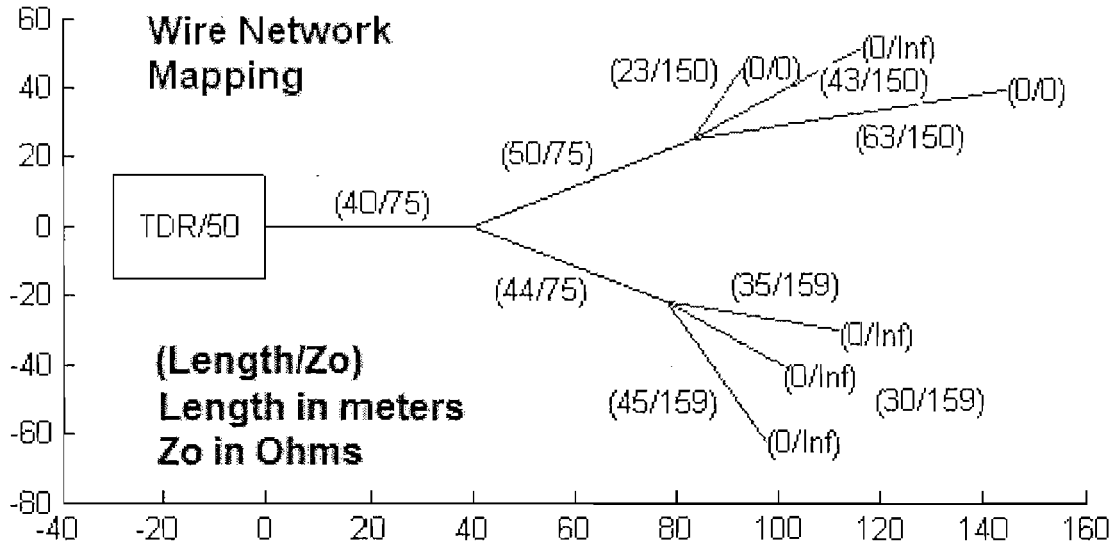

Figure 4-3 Map of the Example Wiring Network

This simulated TDR data is plotted in Figure 4-4. The level of the test signal is indicated that has been input into the wire network. The reflections seen at the TDR probe are indicated in the plot. The plot looks very complicated and somewhat difficult to read. But if we look closer at point A (Figure 4-5) we can see the first reflection from the termination furthest away from the source appearing at the TDR probe. This point is at about 306m in the plot, because of the signal traveling twice the distance (into the network and back). This was determined from the model vector. Starting at the input to the wire network the signal proceeds along the 40m wire, then branches into the 50m wire and again branches into the 63m wire and terminates on a short circuit. It then returns along the same three wires into the TDR measuring equipment. The rest of the

data points after point A are different multiple reverberations in the wiring network. Knowledge of reverberations shows that the network can be found with only a subset of the TDR data.

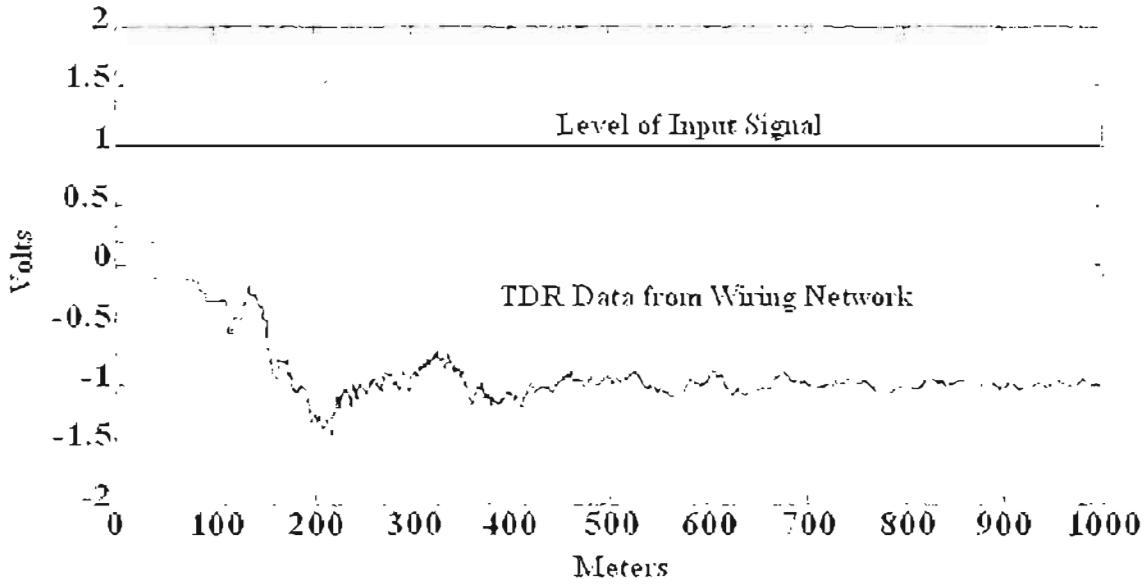

Figure 4-4 Wire Network - TDR Data

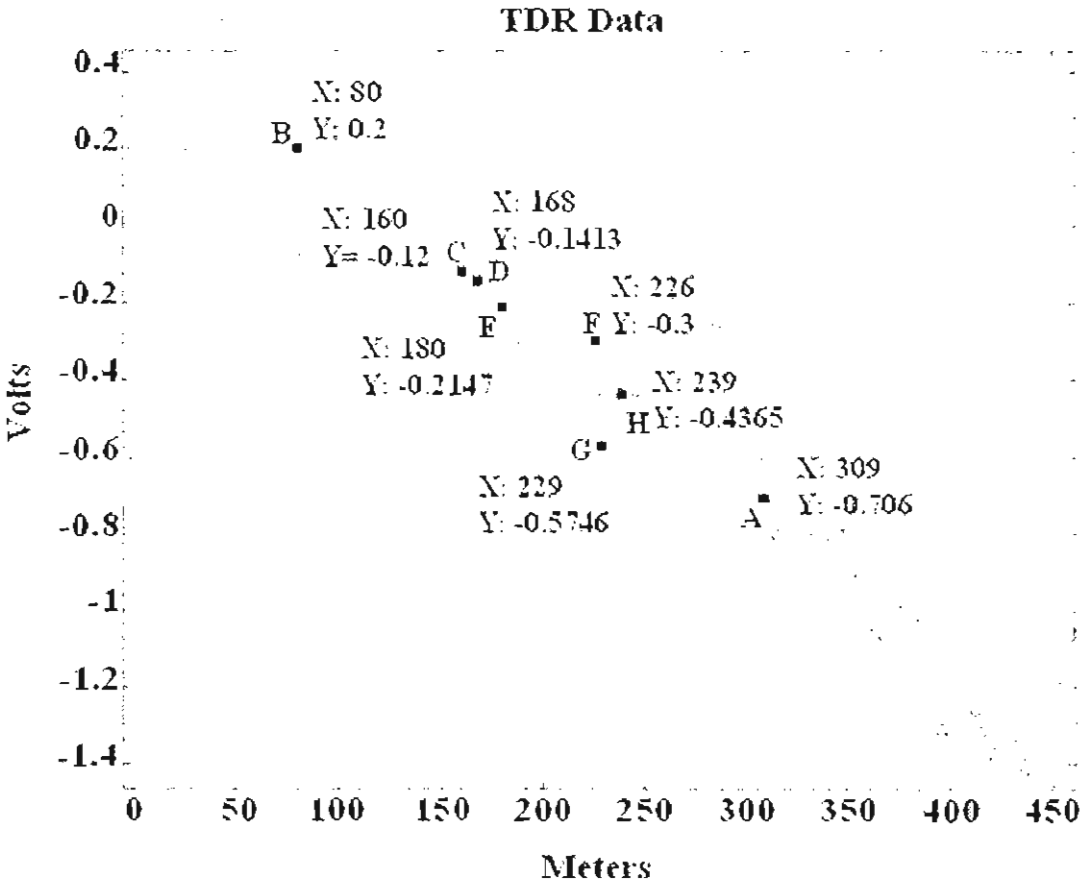

Figure 4-5 Closer in Input TDR data

4.4 Wire Mapping Process

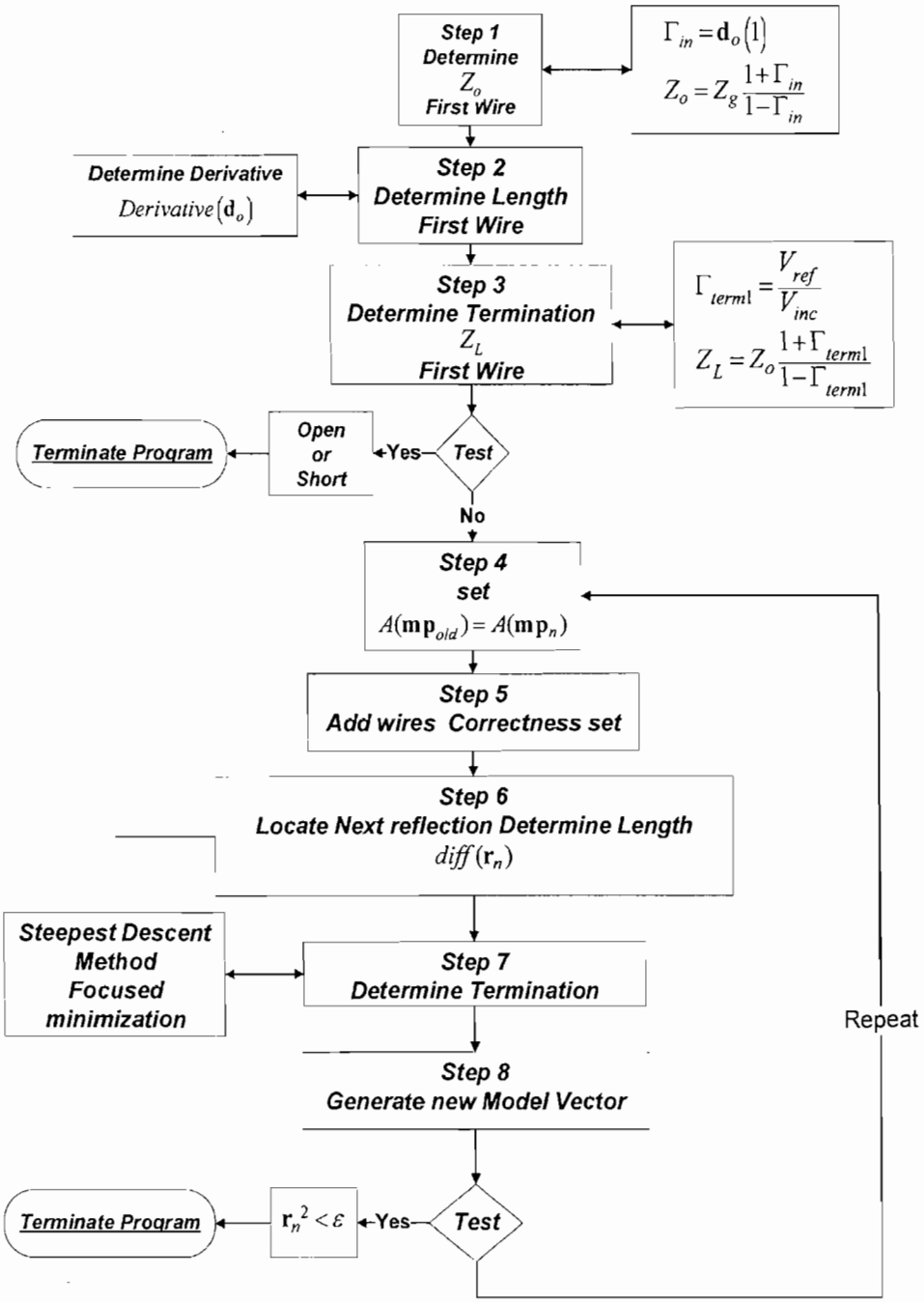

Figure 4-6 Program Algorithm

4.4.1 Step 1: Determination of Z_o of the First Wire

If the data shown in Figure 4-7 are examined closely a number of steps in the voltage plot may be seen.. Point A is still labeled as before. The initial steps in the TDR data provide a simple way to compute the impedance of the first wire without using minimization methods (it will be used on other wire branches). The start of the plot has an initial voltage level of 0.2V (to the left of point B, Figure 4-7), which is V_{refl} with an

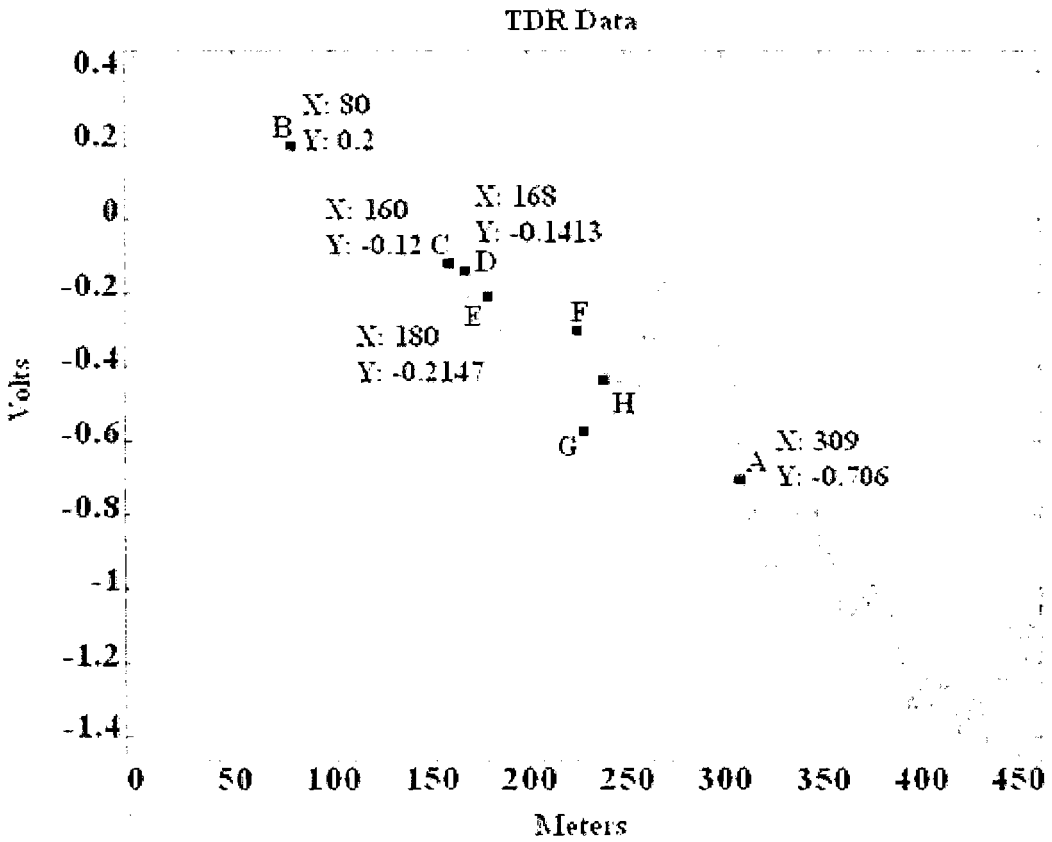

Figure 4-7 Magnified - TDR Data

initial voltage V_{inc} = 1.0V. The reflection coefficient at the input to the wire network is calculated

$$\Gamma_{in} = \frac{V_{refl}}{V_{inc}} \tag{4.5}$$

$$\Gamma_{in} = \frac{0.2}{1.0} = 0.2 \tag{4.6}$$

and used to find the characteristic impedance of the first wire, assuming a generator impedance of 50 ohms:

$$Z_o = (50\Omega)\frac{1+0.2}{1-0.2} = 75\Omega \tag{4.7}$$

4.4.2 Step 2: Determination of the Length of the First Wire

– Derivative of TDR Data

The length of the transmission line is found by taking the derivative of the TDR data and locating point B as shown in Figure 4-8 . The length of the first wire is $80m/2 = 40m$, where the factor of 2 accounts for the wave moving from the source to the termination and back again. In this way parameters of the first line have been found with minimal effort and will be provided to the inversion algorithm as a priori

information (using A as the starting point).

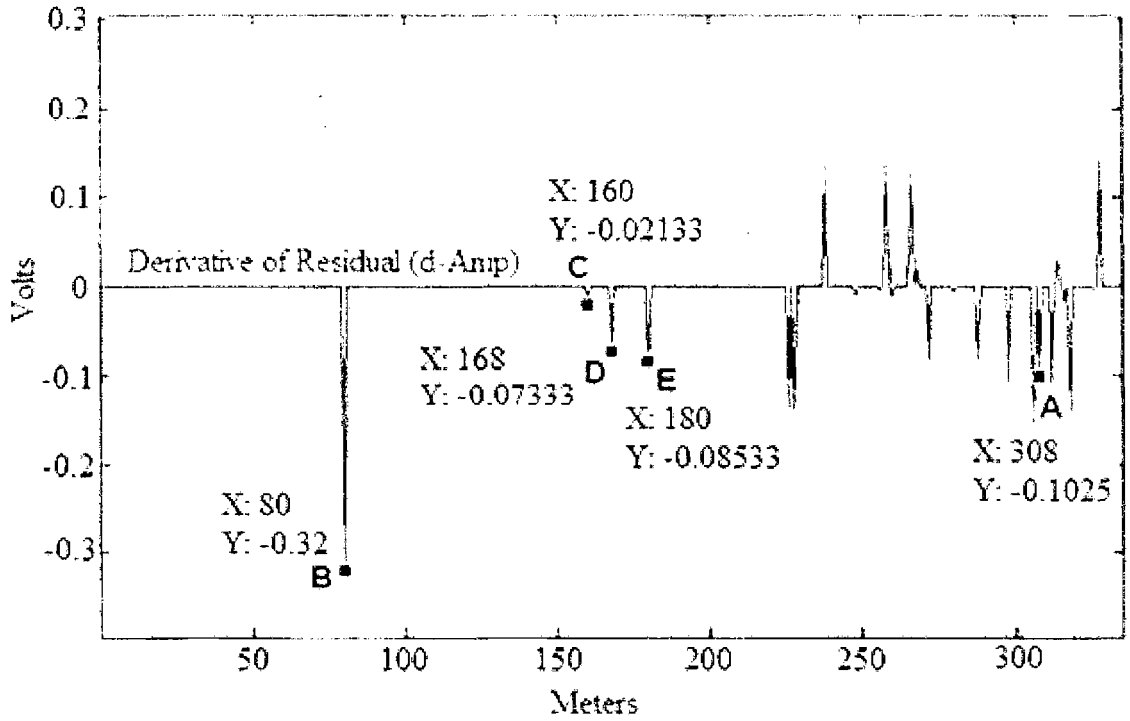

Figure 4-8 Derivative of Input TDR Data

Observation: In the close up of the TDR data in Figure 4-7 it appears that point C is related to point B, since the distance traveled to point C is a multiple of the distance traveled to point B. If this is the case, point C will be removed by the residual.

4.4.3 Step 3: Determination of the Termination of the First Wire

The next parameter to be found is the termination on the first wire. This is also found from the TDR data. The incident wave on the termination is given by

$$\Gamma_{term} = \frac{V_{reflect\_term}}{V_{inc\_term}}$$

$$Z_{term} = Z_o \frac{1+\Gamma_{term}}{1-\Gamma_{term}} \tag{4.8}$$

$V_{inc\_term} = 1+\Gamma_{in}$ which equals 1.2V for this example, and $V_{reflect\_term}$ is $\Gamma_{term} T_g$ (found from the difference in the voltage levels at point A and point B in Figure 4-9) divided by the T_g transmission coefficient. This transmission coefficient is given by

$$T_g = \frac{2Z_g}{Z_g + Z_o} \tag{4.9}$$

Z_o has already been found and Z_g was given as 50Ω. Thus $T_g = 0.8$, $V_{reflect\_term} = 0.4V$.

With this information Γ_{term} and Z_{term} can be determined.

$$\Gamma_{term} = \frac{0.4}{1.2} = 0.3333$$

$$Z_{term} = 75\Omega \frac{1-0.333}{1+0.333} = 37.50\Omega \tag{4.10}$$

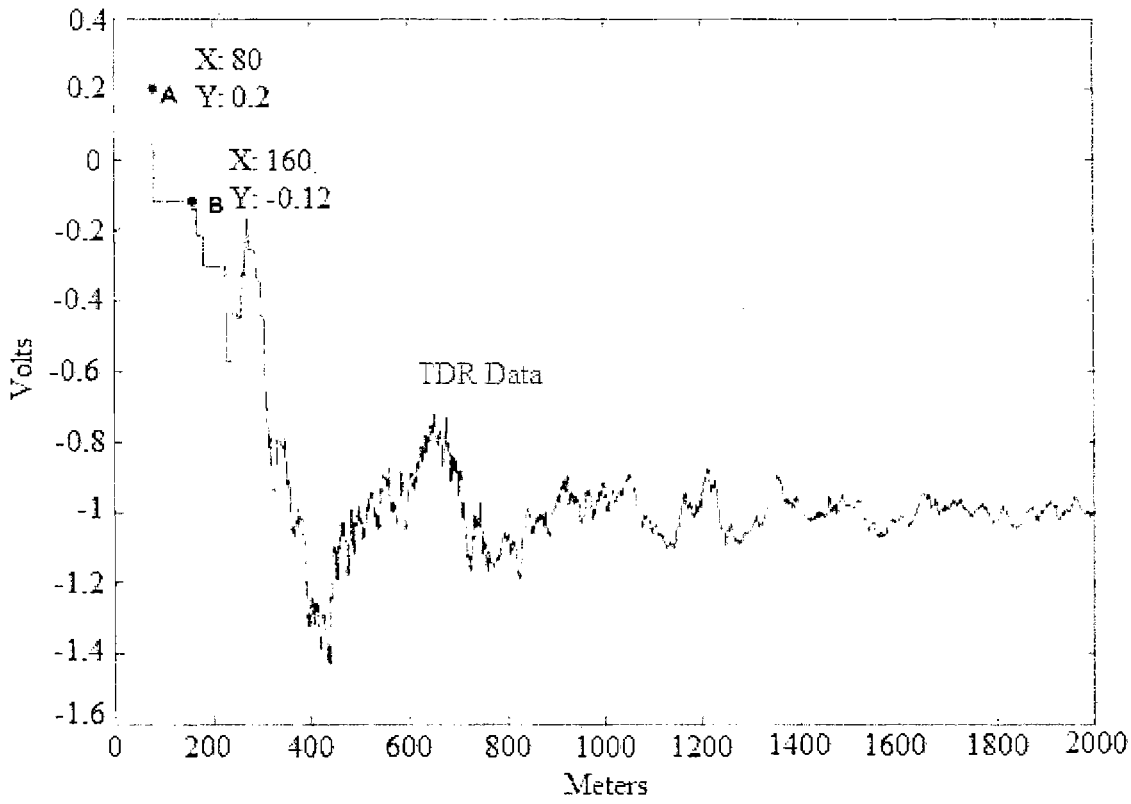

Figure 4-9 TDR Data Focused on A and B

4.4.4 Step 4: Generation of Model Vector for the First Wire

Generating the starting parameter vector mp_1 has been shown in section 3.1.1. We have determined these parameters for the first wire (Z_o, length, Z_L). The parameter vector is constructed remembering that the first parameter is set to 1 for a TDR type data output of the forward operator (Figure 3-2). This parameter vector would be configured as $[1\ L_1\ Z_1\ \#W\ 0\ T_1\ 0]$, so with $L_1 = 40m$, $Z_o = 75\Omega$, $\#W = 1$, and $T_1 = 37.5\Omega$ mp_1 can be generated (leaving off any units).

$$mp_1 = [1\ 40\ 75\ 1\ 0\ 37.5\ 0] \tag{4.11}$$

This parameter vector is then applied to the forward operator, and its TDR response is shown in Figure 4-10 and labeled intermediate. The input TDR data $\mathbf{d}_o$ has been plotted with the first wire and its termination via the forward operator $A(*)$. The first wire's TDR response overlaps the first part of the input TDR data $\mathbf{d}_o$. This forward operation

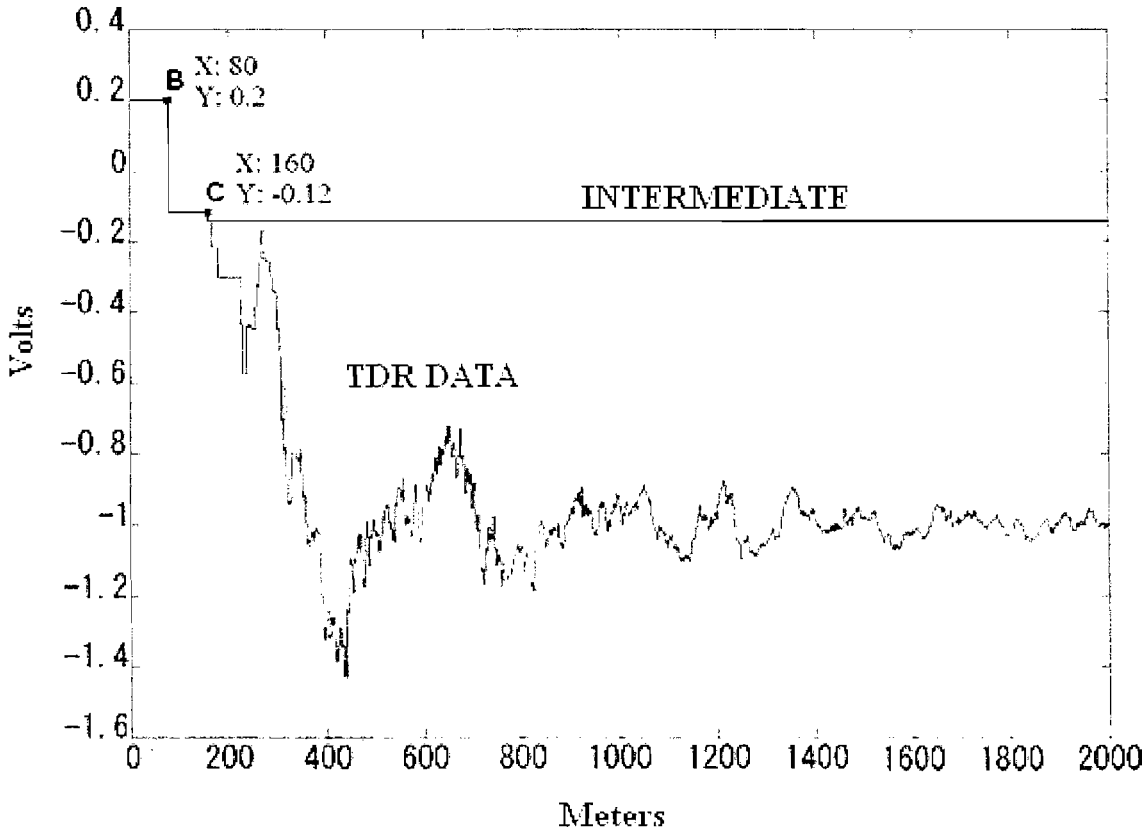

Figure 4-10 Intermediate mp TDR Data Plotted

$A(mp_1)$ includes the primary and secondary reflections of the first wire due to the 37.5Ω termination and the 75Ω characteristic impedance of the transmission line. These reflections are removed (Points A and B) from $\mathbf{d}_o$ through the use of the residual $\mathbf{d}_o - A(\mathbf{m}_n)$. This will allow analysis of later sections of the transmission line using all new residuals of the input TDR data. This first residual is plotted in red in Figure 4-11.

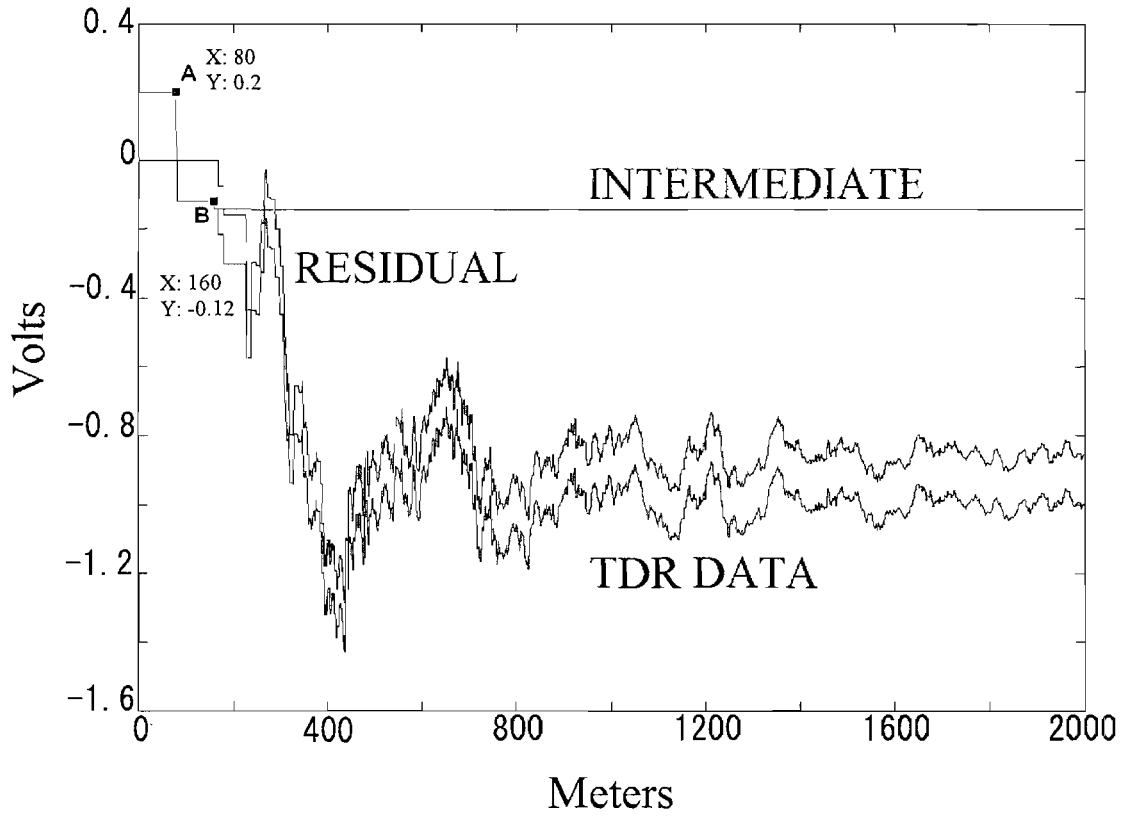

Figure 4-11 Intermediate Residual

4.4.5 Step 5: Wires Are Added from the Correctness Set

We now seek the next impedance discontinuity. To do this we have to add to the model vector mp_1 wires that represent the 37.5Ω terminating impedance. These transmission lines are connected in parallel to the first transmission line. The wires are found using the correctness set, which is a lookup table listing all the allowable terminating impedances and what configuration of additional wires and their associated characteristic impedances that would result in the expected terminating impedance. In this example the 37.5Ω impedance is caused by two parallel 75Ω transmission lines. These two additional wires are set in the place of the termination of mp_1 (the first wire model vector), which changes the #W parameter in mp_1 from 1 to 2. This gives mp_2. The new wires would be added as in equation (4.12).

$$mp_2 = [1\ 40\ 75\ 2\ \mathrm{Len}_1\ 75\ 1\ \mathrm{Len}_2\ 75\ 1\ 0\ \mathrm{T}_1\ 0\ 0\ \mathrm{T}_2\ 0] \tag{4.12}$$

4.4.6 Step 6: The Next Reflection Is Located from the Residual (4.4.4)

The first residual has been plotted in Figure 4-12. Taking the derivative of the residual (Figure 4-12) gives the plot of Figure 4-13. The shortest length of the two wires added in step 5 (4.4.5) is found next from the data of Figure 4-13, the first discontinuity at point A, using the derivative of the residual.

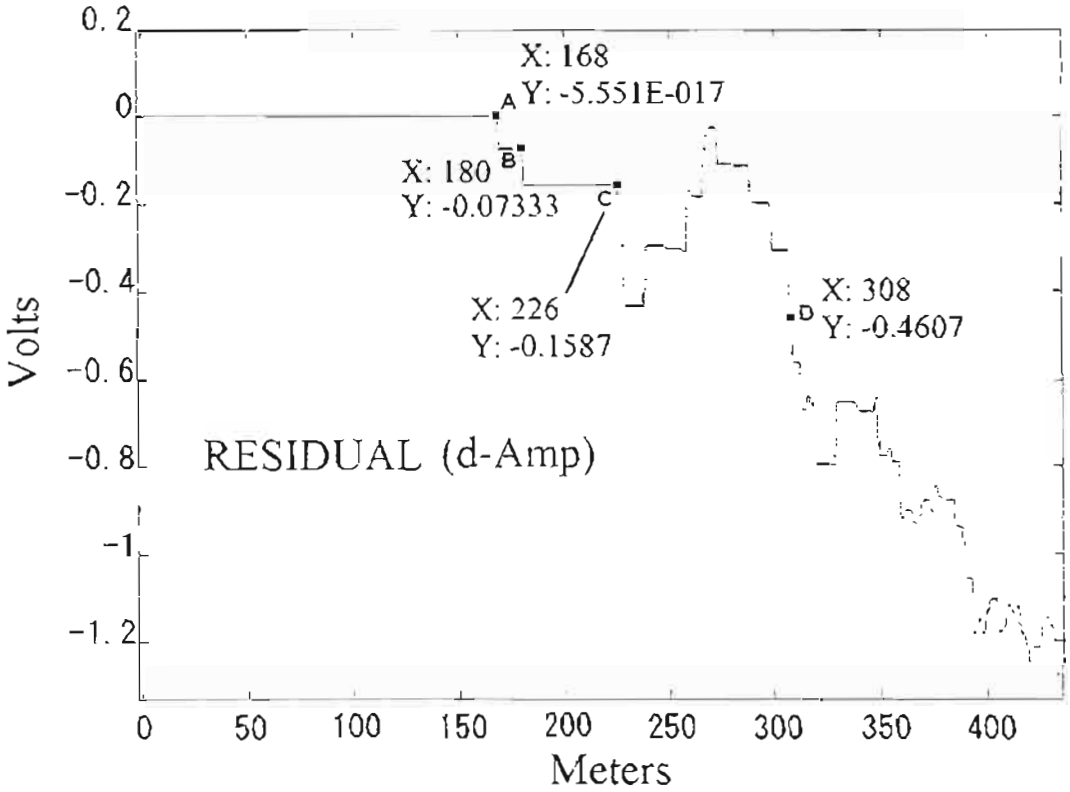

Figure 4-12 Residual TDR Data

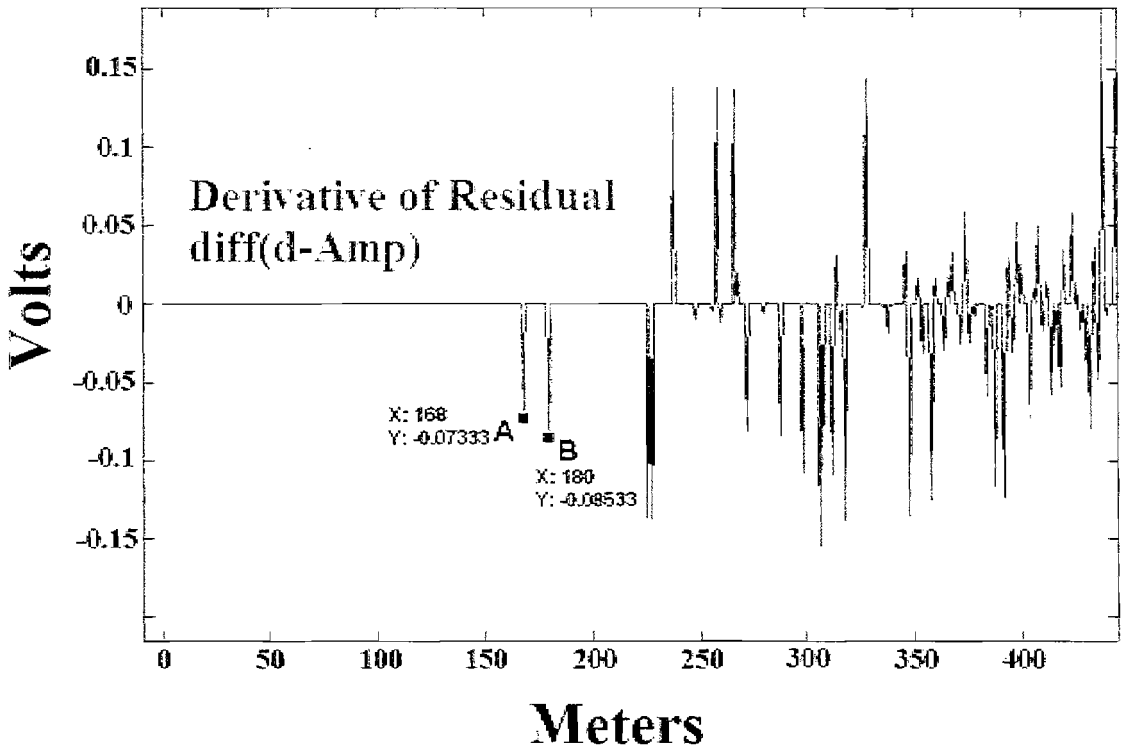

Figure 4-13 Derivative of the Residual

The distance to point A (starting at the input to the wiring network) of 168m (Figure 4-13) is twice the distance to the end of one of the two newly added wires. Recall that part of the distance traveled is taken up by the length of the first wire. We have therefore $168m/2 = 84m$ (point A) minus the length of the first wire (40m), $84m - 40m = 44m$, yielding the length of the shortest wire. We can count on this number being correct, because reflections from any shorter lines have been removed from the input data through the use of the residual.

We have yet to determine which of the two lines has the length of $44m$. This is

not an issue here, because the two lines that were added have the same characteristic impedance, so it does not matter which one is given the length.

The second discontinuity (point B Figure 4-13) could be correct, or it could be a secondary reflection of the wire just found. So the length of the second wire would be set to a length that would remove its effects far away from the wire length already found in this step. The addition of two wires to the first wire is then modeled in the parameter vector mp_2 with $\text{Len}_1 = 44m$ and $\text{len}_2 = 300m$ 300m is arbitrary and could be any length significantly greater than Len_1. The purpose of this is to move the predicted reflections from Len_2 far enough from those of Len_1 that they do not overlap or interfere and therefore Len_1 should be determined before proceeding to determination of Len_2. Equation (4.12) would be changed with this new information to

$$mp_2 = [1\ 40\ 75\ 2\ 44\ 75\ 1\ 300\ 75\ 1\ 0\ T_1\ 0\ 0\ T_2\ 0] \tag{4.13}$$

4.4.7 Step 7: Terminations

The initial terminations on each wire can be derived from the polarity of points A and B. Negative polarities are caused by shorts or low impedances, and positive polarities are caused by open circuits or high impedances. With the second wire set sufficiently long to move its reflections away from the shorter wire, the termination of this shorter wire (length of 44m) can be evaluated. If this termination is not a short, the

terminating impedance is found by using the steepest descent method to minimize the voltage reflection seen at the source. The steepest descent method looks at the voltage at one point (in this example point A Figure 4-13). Point A contains the reflection and any transmissions from or through any impedance discontinuities that the voltage wave experiences in its travel in the wiring network.

In the case of our example the terminating impedance found in this step would be 53Ω, and this termination would be placed in the mp_2 model vector as shown below

$$mp_2 = [1\ 40\ 75\ 2\ 44\ 75\ 1\ 300\ 75\ 1\ 0\ 53\ 0\ 0\ T_2\ 0] \tag{4.14}$$

4.4.8 Step 8: Generation of a New Model Vector

Vector parameter mp_2 would be found in this step. Since the termination is neither an open nor a short circuit the termination of 53Ω is a combination of parallel transmission lines. The impedance of 53Ω indicates that there must be three wires of 159Ω in parallel ($159\Omega / 3 = 53\Omega$) chosen from the correctness set. The add wire step is again used with the resulting model vector being expanded to

$$\begin{aligned} mp_3 = [&1\ 40\ 75\ 2\ 44\ 75\ 3\ 300\ 75\ 1\ 300\ 159\ 1\ 300\ 159\ 1 \\ &300\ 159\ 1\ 0\ 0\ 0\ T_2\ 0\ 0\ T_3\ 0\ 0\ T_4\ 0] \end{aligned} \tag{4.15}$$

The length of 300m is again used to move the reflections due to these wires and

terminations away from the area of the next discontinuity. Setting mp_{old} to mp_2 a new residual is computed using mp_{old} . This gives $\mathbf{r}_2 = \mathbf{d}_o - A(mp_2)$ data with a new point A with the previous wire's reflection and any of its reverberations removed from the new residual. This process continues. The only difference here is that each wire would in turn be set to the new length of wire (next shortest length) with the others set to a length that would remove their reflections from the vicinity of the next shortest length. Terminations would be found that would zero the derivative of the residual at the point of the shortest length line. As each length and termination is found it is placed in the parameter vector mp and its reflections are removed from the next residual. This continues until the square of the norm of the residual is reduced below some predefined number ε.

4.5 Noise

Noise causes spreading in voltage levels in the TDR data. This spreading of the voltage levels results in a variation of allowed impedance determined by the program. With the correctness set defined the program is unable to determine what to do and runs in a continuous loop.

The correctness set needs to be expanded to allow a greater set of impedance values this will allow the set to pick a value closer to the average value of the voltage level of the TDR data. An averaging filter was used to get an average voltage between impedance discontinuities. This filter needs to be fine tuned so as to produce a response

that has the smallest error between the filtered TDR data and the given noise data. This will produce the best results from the mapping algorithm outlined in this thesis.

Lengths of wires are determined from the location of discontinuities in the impulse response of the TDR data. The method works reasonably well with perfect data (no noise) but is not yet robust enough for realistic data with noise included.

With the addition of noise, the data are spread out, giving imprecise impedance levels. Averaging the data helps in reducing the noise effect but is still not enough to make the method run reliably with noisy data. This variation of the impedance level causes numerical errors within the program, necessitating a widening of the allowed impedance levels.

Noise can hide small reflections, making them hard to distinguish from the surrounding noise and thus making the lengths of the wires impossible to determine. If the impedance discontinuity is relatively large, it will be seen through the noise.

4.6 What Can Go Wrong

There are a number of wire networks that could not be resolved by this program. These include:

1) Any wires placed in parallel with resulting impedance values equal to that of the characteristic impedance of the previous transmission line, thus producing no reflection at the junction.
2) Transmission lines in parallel having the same length and identical impedances. These would look like a single transmission line.

4.7 Conclusions

A method has been described that allows the efficient determination of a wire network from its TDR signature. This is due to the understanding that the primary reflection occurs first and that secondary reflections can be removed from the misfit functional as the wiring network model is created. The primary and any secondary reflections are removed leaving behind the next primary reflection of the signal from an impedance discontinuity that has yet to be uncovered and modeled.

The process first finds the characteristic impedance of the first wire, then finds its length, then determines the termination of the wire. If the termination is an open or a short circuit the program terminates. If the termination is something other than an open or a short the algorithm looks to the correctness set to determine the number of wires and their characteristic impedances that should be connected to the first wire.

The model of the first transmission line with its termination is put to the forward operator which generates the simulated TDR data. These simulated data are subtracted from the input TDR data $\mathbf{d}_0$, $A(\mathbf{m})-\mathbf{d}_0$ removing all reflections due to the first wire and it termination. This leaves a residual that contains the reflections of any impedance discontinuities that have as yet not been modeled.

The first impedance discontinuity in the residual is the next wire length and termination to be found. To do this one of the wires terminating the first wire is isolated. There will be other wires in parallel with this isolated wire and there reflections will need to be removed from consideration.

The removal of the effects of the parallel wires is done by moving the wire lengths beyond the length of the isolated wire which length is set to the length found from the first discontinuity of the residual found in the previous step. The termination of the isolated wire is next found using steepest descent method and if the termination is not an open or a short, additional wires are added to this current wire (isolated). Each wire is isolated from the others as needed and the model vector is constructed one wire at a time.

In this way reflections are removed from the TDR data as the wire model is built by using a modified residual $A(\mathbf{m}) - \mathbf{d}_0$ which preserves the polarity of all reflections within the TDR data. The methods works well for perfect TDR data.

If the TDR data are noisy the algorithm fails to find the mapping of the wiring network. The correctness set was determined to be part of the problem and could be expanded and improved in future work.

A trial run of the program was made with the input TDR data simulated by the m vector in (4.16) the program returned the vector mp in (4.17) with the error being returned of r = 9.3858e-015.

$$\begin{aligned} m = [&1\ 40\ 75\ 2\ 50\ 75\ 3\ 44\ 75\ 3\ 23\ 150\ 1\ 43\ 150\ 1\ 63\ 150\ 1\ 35\ 159\ 1\ 30\ 159\ 1\ 45\ 159\ 1 \\ &0\ 0\ 0\ 0\ 999\ 0\ 0\ 0\ 0\ 0\ 999\ 0\ 0\ 0\ 0\ 0\ 999\ 0] \end{aligned} \tag{4.16}$$

$$\begin{aligned} mp = [&1\ 40\ 75\ 2\ 44\ 75\ 3\ 50\ 75\ 3\ 30\ 159\ 1\ 35\ 159\ 1\ 45\ 159\ 1\ 23\ 150\ 1\ 43\ 150\ 1\ 63\ 150\ 1 \\ &0\ 0\ 0\ 0\ 999\ 0\ 0\ 999\ 0\ 0\ 0\ 0\ 0\ 999\ 0\ 0\ 0\ 0] \end{aligned} \tag{4.17}$$

The vectors m and mp are the same except for the order of the elements of the vectors. This was a complex example of the workings of the software developed in this thesis.

APPENDIX

This appendix has been added to introduce the reader to the operations that are allowed on vector spaces. I also have included the *Euclidean Space*. The *Euclidean Space* has all the desirable properties that one would want for the *Hilbert Space*. It has distance, direction (inner product), and vector operations such addition, subtraction etc. This is all important in constructing the "Misfit Functional".

A.1 Euclidean Space - Vector Operations

This represents an n-dimensional vector in an n-dimensional Euclidian Space.

$$\mathbf{a} = \left(a_1, a_2, a_3, \ldots, a_n\right) \tag{A.1}$$

A.1.1 Norm of a Vector

The norm of a vector tells us the length of the vector **a**.

$$\|\mathbf{a}\| = \sqrt{a_1^2 + a_2^2 + a_3^2 + \ldots + a_n^2} \tag{A.2}$$

Its properties are

$$\|\mathbf{a}\|>0 \quad \text{if} \quad \mathbf{a}\neq\mathbf{0}, \quad \|\mathbf{a}\|=0 \quad \text{if} \quad \mathbf{a}=\mathbf{0} \tag{A.3}$$

$$\|\lambda\mathbf{a}\|=|\lambda|\|\mathbf{a}\| \tag{A.4}$$

λ is a scaler

$$\|\mathbf{a}+\mathbf{b}\|\leq\|\mathbf{a}\|+\|\mathbf{b}\| \tag{A.5}$$

A.1.2 Inner Product

The inner product is used to determine the distance between the measured and calculated data in the *Hilbert Space*. As has been mentioned before the *Hilbert Space* has been constructed with many of the properties of the *Euclidian Space*.

The inner product is defined as

$$\mathbf{a}\cdot\mathbf{b}=\sum_{i=1}^{n}a_i b_i \tag{A.6}$$

And its norm is

$$\|\mathbf{a}\|=\sqrt{\mathbf{a}\cdot\mathbf{a}} \tag{A.7}$$

The two vectors are orthogonal if

$$\mathbf{a} \cdot \mathbf{b} = 0 \tag{A.8}$$

A.1.3 Basis

Weighted sums of these vectors describe any vector within this Vector space.

$$\mathbf{e}_1=(1,0,0,\ldots,0),\mathbf{e}_2=(0,1,0,\ldots,0),\mathbf{e}_3=(0,0,1,\ldots,0),\mathbf{e}_n=(0,0,0,\ldots,1),$$

$$\mathbf{a} = a_1\mathbf{e}_1+a_2\mathbf{e}_2+\ldots+a_n\mathbf{e}_n=\sum_{i=1}^{n} a_i e_i$$

$$\mathbf{e}_i \cdot \mathbf{e}_k=0; \quad \text{if} \quad i \neq k, \quad \mathbf{e}_k \cdot \mathbf{e}_k=1, \tag{A.9}$$

$$\mathbf{a} \cdot \mathbf{e}_i=a_i$$

A.1.4 Linear Operators

A.1.4.1 Linear Transformations

$$\mathbf{d}=A(\mathbf{a}) \tag{A.10}$$

$$A\left(\alpha_1\mathbf{a}_1 + \alpha_2\mathbf{a}_2\right)=\alpha_1 A\left(\mathbf{a}_1\right)+\alpha_2 A\left(\mathbf{a}_2\right) \tag{A.11}$$

A linear operator is called a bounded operator if it has a bounded norm.

$$\|A\| < \infty \tag{A.12}$$

A linear bounded operator is a continuous operator, i.e., that small variations of the argument of the operator will result in small variations in the operator itself.

$$\|A(\mathbf{a}) - A(\mathbf{b})\| = \|A(\mathbf{a}-\mathbf{b})\| \le \|A\|\|\mathbf{a}-\mathbf{b}\| \tag{A.13}$$

Therefore, if $\|\mathbf{a}-\mathbf{b}\| < \delta = \frac{\varepsilon}{\|A\|}$, then $\|A(\mathbf{a}) - A(\mathbf{b})\| < \varepsilon$

In a finite dimensional space any linear operator is bounded and continuous.

A.1.4.2 Linear Functionals

A functional in Euclidean space is a rule that unambiguously assigns a single real number to any element in the space E_n. The functional is linear if for any vector $\mathbf{a}_1, \mathbf{a}_2 \in E_n$ and any scalars $\alpha_1, \alpha_2 \in E_1$ we have

$$f(\alpha_1\mathbf{a}_1 + \alpha_2\mathbf{a}_2) = \alpha_1 f(\mathbf{a}_1) + \alpha_2 f(\alpha_2\mathbf{a}_2) \tag{A.14}$$

The norm of the functional is

$$\left|f(\mathbf{a})\right| \le \|f\|\|\mathbf{a}\| \tag{A.15}$$

A.2 Functional Spaces

A.2.1 Metric

The metric introduces a "distance" between two data sets.

$$\mu(\mathbf{h},\mathbf{g}) \text{ distance between } \mathbf{h} \text{ and } \mathbf{g} \tag{A.16}$$

$$\mu(\mathbf{h},\mathbf{g}) = 0 \Leftrightarrow \mathbf{h} = \mathbf{g} \tag{A.17}$$

$$\mu(\mathbf{h},\mathbf{g}) = \mu(\mathbf{g},\mathbf{h}) \tag{A.18}$$

$$\mu(\mathbf{h},\mathbf{g}) \le \mu(\mathbf{h},\mathbf{q}) + \mu(\mathbf{q},\mathbf{g}), \text{ for any } \mathbf{h},\mathbf{g},\mathbf{q} \in M \tag{A.19}$$

(Triangle inequality)

A.2.2 Linear Vector Space

In a linear vector space a number of operations are legal:

$$\mathbf{f}+\mathbf{g}=\mathbf{g}+\mathbf{f} \tag{A.20}$$

$$\mathbf{f}+(\mathbf{g}+\mathbf{h})=(\mathbf{f}+\mathbf{g})+\mathbf{h} \tag{A.21}$$

$$\mathbf{0} \in L;\ \ \mathbf{f}+\mathbf{0}=\mathbf{f} \tag{A.22}$$

$$(\alpha+\beta)\mathbf{f}=\alpha\mathbf{f}+\beta\mathbf{f} \tag{A.23}$$

$$\alpha(\beta\mathbf{f})=(\alpha\beta)\mathbf{f} \tag{A.24}$$

$$\alpha(\mathbf{f}+\mathbf{g})=\alpha\mathbf{f}+\alpha\mathbf{g} \tag{A.25}$$

$\alpha,\beta\in E_1,\ \mathbf{f},\mathbf{g}\in L$

$\mathbf{0}$ is the zero element

A.2.3 Normed Linear Space

Has a distanced defined between points of the space.

$$\|\mathbf{f}\|\geq 0,\ \text{and}\ \|\mathbf{f}\|=0\Leftrightarrow\mathbf{f}=\mathbf{0} \tag{A.26}$$

$$\|\alpha\mathbf{f}\|=|\alpha|\|\mathbf{f}\|,\ \alpha\in E_1 \tag{A.27}$$

$$\mu(\mathbf{h},\mathbf{g})=\|\mathbf{f}-\mathbf{g}\| \tag{A.28}$$

A.2.4 Hilbert Space

Linear normed space equipped with the inner product is called a Hilbert space if it is complete.

$$(\mathbf{f},\mathbf{g})=(\mathbf{g},\mathbf{f}) \tag{A.29}$$

$$(\mathbf{f}+\mathbf{g},\mathbf{h})=(\mathbf{f},\mathbf{h})+(\mathbf{g},\mathbf{h}) \tag{A.30}$$

$$(\alpha \mathbf{f}, \mathbf{g}) = \alpha (\mathbf{f}, \mathbf{g}) \tag{A.31}$$

$$(\mathbf{f}, \mathbf{f}) > 0 \tag{A.32}$$

$$(\mathbf{f}, \mathbf{f}) = 0 \Leftrightarrow \mathbf{f} = \mathbf{0} \tag{A.33}$$

This space has geometrical properties. Not only is there a distance between any two vectors, but also an angle between the vectors:

$$\cos\phi = \frac{(\mathbf{f}, \mathbf{g})}{\|\mathbf{f}\| \|\mathbf{g}\|} \tag{A.34}$$

Two elements $\mathbf{f}$ and $\mathbf{g}$ of a Hilbert Space are orthogonal if

$$(\mathbf{f}, \mathbf{g}) = 0 \tag{A.35}$$

Every non-zero Hilbert space contains a basis.

A.2.5 Complex Euclidean and Hilbert Space

If the *Hilbert Space* is complex the operations below are changed so that the inner product continues to have the same properties as it does within a real *Hilbert Space* or *Euclidian Space*

$$\|\mathbf{a}\| = \sqrt{|\alpha_1|^2 + |\alpha_2|^2 + |\alpha_3|^2 + \ldots + |\alpha_n|^2} \tag{A.36}$$

$$\mathbf{a} \cdot \mathbf{b} = \sum_{i=1}^{n} a_i b_i \tag{A.37}$$

$$(\mathbf{a}, \mathbf{b}) = (\mathbf{b}, \mathbf{a})^* \tag{A.38}$$

$$(\mathbf{a}, \alpha\mathbf{b}) = (\alpha\mathbf{b}, \mathbf{a})^* = \alpha^* (\mathbf{b}, \mathbf{a})^* = \alpha^* (\mathbf{a}, \mathbf{b}) \tag{A.39}$$

REFERENCES

[1] C. Furse, Y. C. Chung, C. Lo, and P. Pendayala, "A critical comparison of reflectometry methods for location of wiring faults," Journal of *Smart Structures and Systems*, vol. 2, no.1, 2006, pp. 25-46, Techno Press, South Korea.

[2] L. A. Griffiths, R. Parakh, C. Furse, and B. Baker, "The invisible fray: a critical analysis of the use of reflectometry for fray location," *IEEE Journal of Sensors* vol. 6, pp. 697-706, 2006.

[3] K. Nagoti, "Mapping of network topologies using reflectometry methods," MS: *Electrical and Computer Engineering,* Salt Lake City, University of Utah, 2004

[4] A. Mahoney, C. Lo, Y. C. Chung, and C. Furse, "Use of genetic algorithms and reflectometry for identification of network topologies," *IEEE Trans Electromagnetic Compatibility.* Personal Communication C. Furse 2005

[5] M. S. Zhdanov, *Geophysical inverse theory and regularization problems* 1st ed. Amsterdam, The Netherlands: Elsevier Science B.V., 2002.

[6] M. R. Spiegel, "Calculus of finite differences and difference equations," *Schaum's Outlines,* p. 259, 1971.

[7] S. Yakowitz and F. Szidarovszky, *An Introduction to numerical computations*, 1st ed. New York: Macmillan Publishing Company, 1986.

[8] C. Lo and C. Furse, "Modeling and simulation of branched wiring network," Personal Communication C. Furse 2005